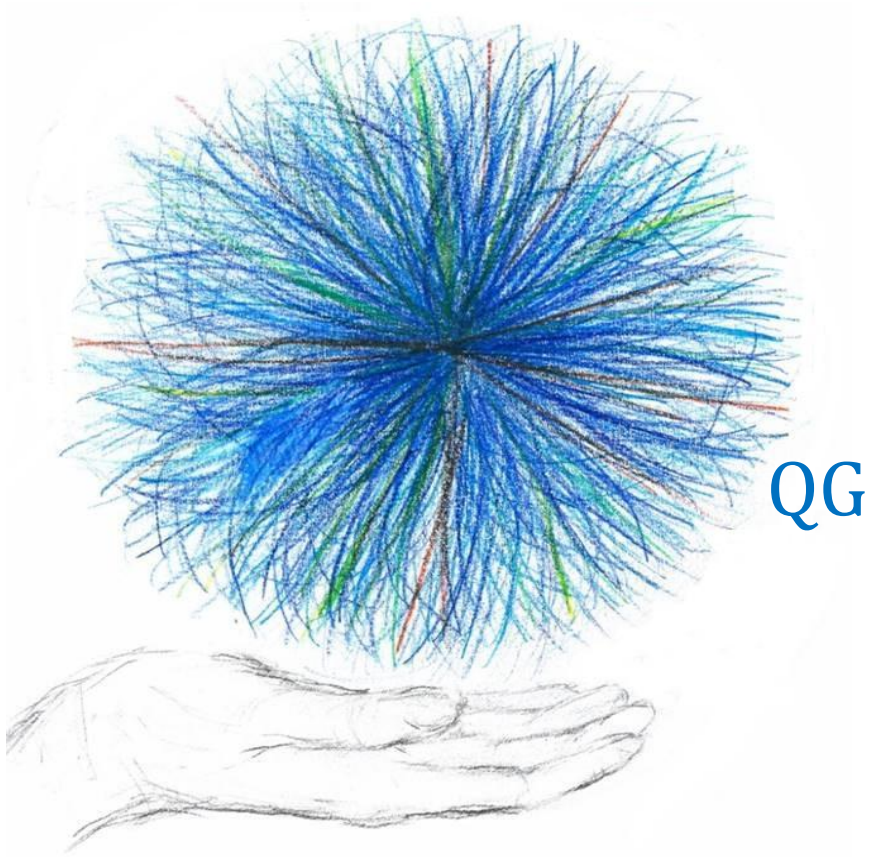

QGP tomography: from qhat and quasiparticles to Bayesian inference and jets

Magdalena Djordjevic,

In collaboration with: Marko Djordjevic, Bithika Karmakar, Dusan Zigic, Bojana Ilic, Igor Salom, Jussi Auvinen and Pasi Huovinen

European Research Council

МИНИСТАРСТВО ПРОСВЕТЕ, НАУКЕ И ТЕХНОЛОШКОГ РАЗВОЈА

Motivation

- Energy loss of high-pt light and heavy particles traversing the QCD medium is an excellent probe of QGP properties.
- Theoretical predictions can be compared with a wide range of data from different experiments, collision systems, collision energies, centralities, and observables.
- Can be used jointly with low-pt theory and experiments to study the properties of created QCD medium, i.e., for precision QGP tomography.

The dynamical energy loss formalism

Has the following unique features:

- *Finite size finite temperature* QCD medium of *dynamical* (moving) partons.
- Based on finite *T* field theory and generalized HTL approach.
- Same theoretical framework for both radiative and collisional energy loss.
- Applicable to both light and heavy flavor.
- Finite magnetic mass effects (M. D. and M. Djordjevic, PLB 709:229 (2012))
- Running coupling (M. D. and M. Djordjevic, PLB 734, 286 (2014)).
- Relaxed soft-gluon approximation (B. Blagojevic, M. D. and M. Djordjevic, PRC 99, 024901, (2019)).
- Included higher-order in opacity effects (S. Stojku, B. Ilic, I. Salom, MD, PRC in press, (2023)).
- No fitting parameters in the model.
- Temperature as a natural variable in the model.

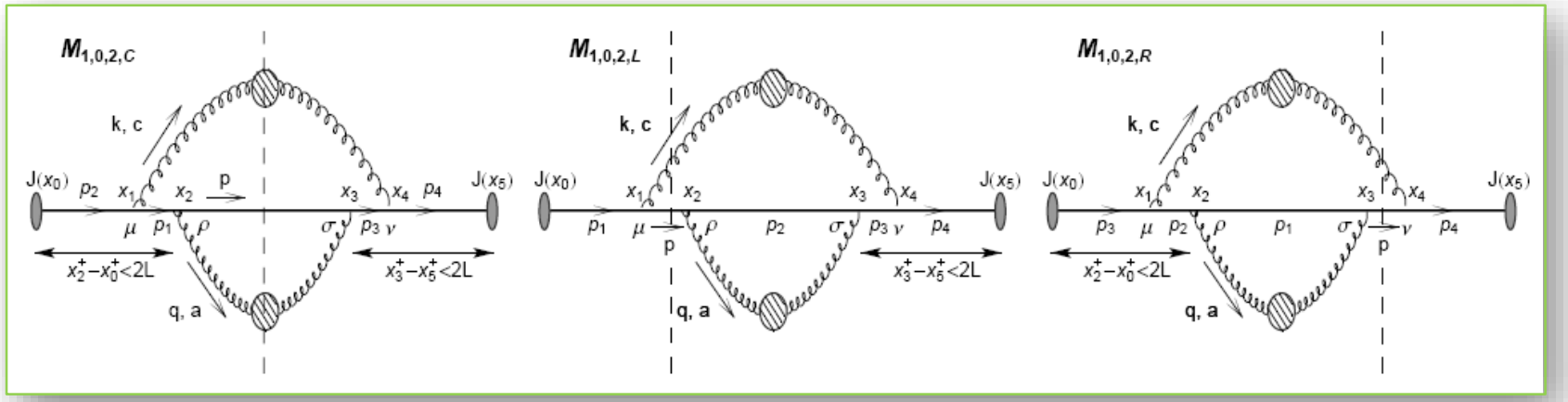

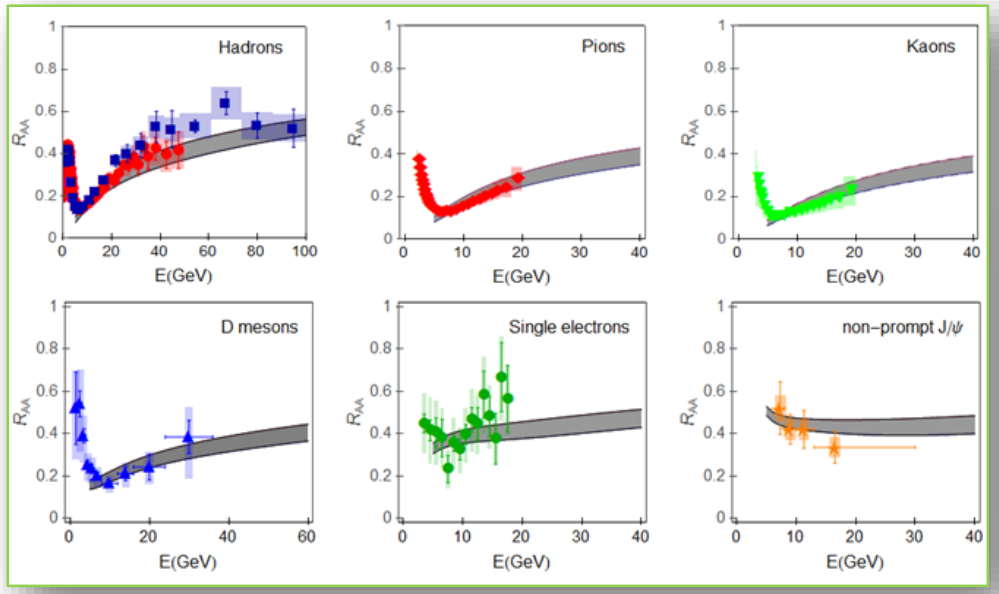

Explains high-pt R_{AA} data for different probes, collision energies, and centralities.

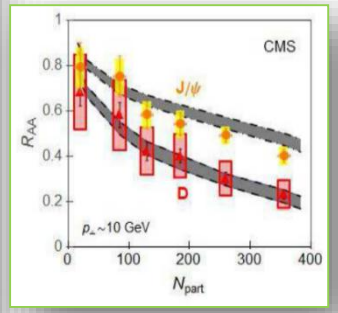

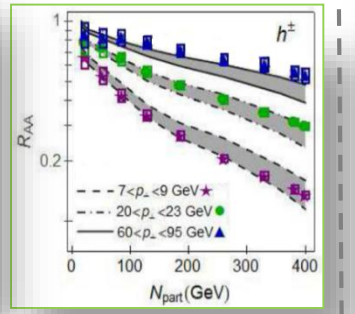

Resolved the longstanding "heavy flavor puzzles at RHIC and LHC".

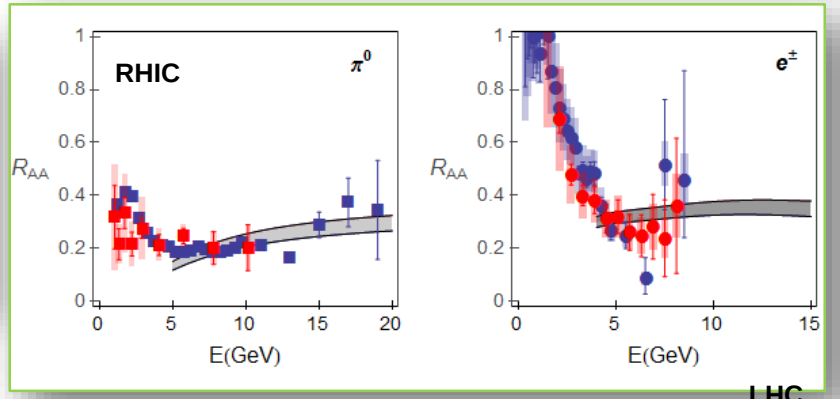

Clear predictive power!

M.D. et al., PRC 92 (2015)

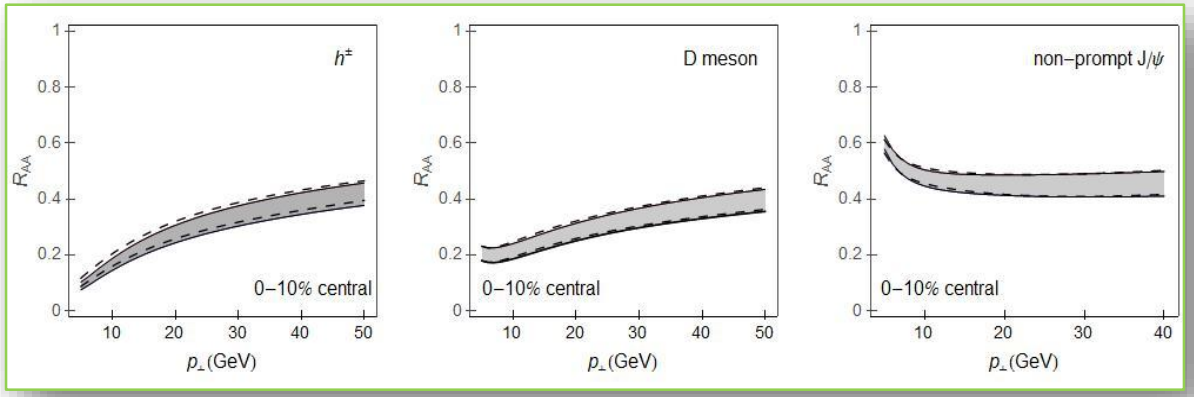

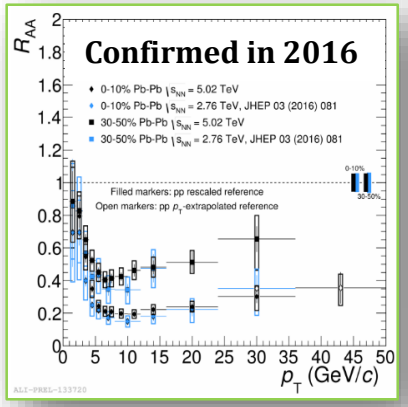

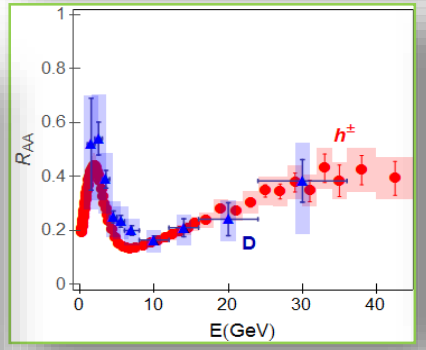

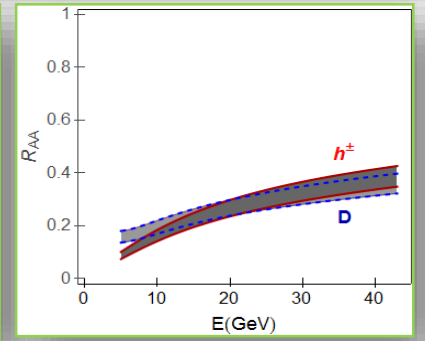

M.D., PRL 112, 042302 (2014)

A realistic description for parton-medium interactions!

Suitable for QGP tomography!

Part I: Can we use dynamical energy loss to constrain η/s?

- Low-$p_\perp$ observables are widely used to explore the bulk QGP properties.
- η/s is well constrained by Bayesian analyses in the low-$p_\perp$ sector in the temperature range $T_c \lesssim T \lesssim 1.5T_c$, but weakly constrained at larger temperatures.
- QGP is expected to behave as a weakly interacting gas - Weakly coupled.
- Fluid dynamics predicts the η/s to be very low - Strongly coupled.
- QGP may behave as perfect fluid near T_c (soft regime), and η/s may increase at high temperatures (hard regime).
- Testing the soft-to-hard hypothesis is difficult: Anisotropy is weakly affected by the η/s at high temperatures.
- High-$p_\perp$ data/theory can serve as a complementary tool.
- Can we constrain η/s by using the dynamical energy loss?

Constraining η/s from the dynamical energy loss $\hat{q}$

Dynamical energy loss:

Capable of accurately reproducing observed R_{AA} without fitting parameters.

Can adequately describe interactions between high-pt particles and the QCD medium.

Reasonable to estimate (η/s)(T) theoretically using the dynamical energy loss model.

Need to estimate the jet quenching parameter $\hat{q}$.

Crucial for assessing interaction strength between jet partons and nuclear matter.

Quantifies the transverse momentum broadening of fast parton due to its elastic scatterings with the medium.

Valuable tool for various purposes:

- Insight into jet quenching phenomena.
- Estimation of bulk medium property (η/s).
- In a weakly coupled limit: $\eta/s \approx 1.25 \frac{T^3}{\hat{q}}$

(Majumder, Muller, Wang, PRL 99, 2007).

Derivation of $\hat{q}$ from the dynamical energy loss

- In dynamical perturbative QCD medium, the interaction between high-pt partons and QGP constituents can be characterized by:

$$\frac{d\Gamma_{el}}{d^2q} = 4C_A\left(1+\frac{nf}{6}\right)T^3\frac{\alpha_s^2}{q^2\left(q^2+\mu_E^2\right)}$$

- After including running coupling and finite magnetic mass, the elastic collision rate becomes:

$$\frac{d\Gamma_{el}}{d^2q} = \frac{C_A}{\pi}T\alpha(ET)\frac{\mu_E^2-\mu_M^2}{(q^2+\mu_E^2)(q^2+\mu_M^2)}$$

- Debye mass is obtained by self consistently solving the following equation (W-Lambert function (Peshier, hep-ph/0601119):

$$\mu_E^2 = \left(1+\frac{n_f}{6}\right)4\pi\alpha\left(\mu_E^2\right)T^2 \qquad \mu_E = \sqrt{\Lambda^2\frac{\xi(T)}{W(\xi(T))}}$$

$$\alpha(t) = \frac{4\pi}{\left(11-\frac{2}{3}n_f\right)}\frac{1}{\ln\left(\frac{t}{\Lambda^2}\right)} \qquad \xi(T) = \frac{1+\frac{n_f}{6}}{11-\frac{2}{3}n_f}\left(\frac{4\pi T}{\Lambda}\right)^2$$

- In the fluid rest frame, weakly dependent on E!

$$\begin{aligned}\hat{q} &= \int_0^{\sqrt{6ET}} d^2q\, q^2\cdot\frac{d\Gamma_{el}}{d^2q}\\ &= C_AT\alpha(ET)\int_0^{6ET}dq^2\,q^2\left(\frac{1}{q^2+\mu_M^2}-\frac{1}{q^2+\mu_E^2}\right)\\ &= C_AT\alpha(ET)\left(\mu_E^2\ln\left[\frac{6ET+\mu_E^2}{\mu E^2}\right]-\mu_M^2\ln\left[\frac{6ET+\mu_M^2}{\mu_M^2}\right]\right)\end{aligned}$$

- In the limit of $ET\to\infty$, reduces to the expression independent of jet energy: $x_{ME}=\mu_M/\mu_E$

$$\hat{q} = C_A\left(\frac{4\pi}{11-\frac{2}{3}n_F}\right)^2\frac{4\pi\left(1+\frac{n_F}{6}\right)}{W(\xi(T))}\left(1-x_{ME}^2\right)T^3$$

- **Expected behavior:** as a property of the medium $\hat{q}$ should be independent (or weakly dependent) on jet energy.

B. Karmakar, D. Zigic, I. Salom, J. Auvinen, P. Huovinen, M. Djordjevic and MD, PRC **108**, 044907 (2023).

What we expect from previous knowledge?

- Sensitive to the coupling strength in QGP: weak coupling enlarges η/s and reduces $\frac{\hat{q}}{T^3}$, and vice versa for strong coupling.
- A rise in $\frac{\hat{q}}{T^3}$ near T_c is predicted to be essential for explaining high-$p_\perp$ v_2. (Liao&Shuryak, PRL 102, 2009).
- In the weakly coupled regime (Majumder, Muller, Wang, PRL 99, 2007) $\eta/s \approx 1.25\frac{T^3}{\hat{q}}$.
- At large T, weakly coupled system.
- Near T_c, strongly coupled limit, and $\frac{T^3}{\hat{q}}$ should significantly deviate from η/s.
- **Soft-to-hard boundary:** the transition region from strong to weak coupling.

η/s and $\frac{\hat{q}}{T^3}$ are key transport coefficients in QGP.

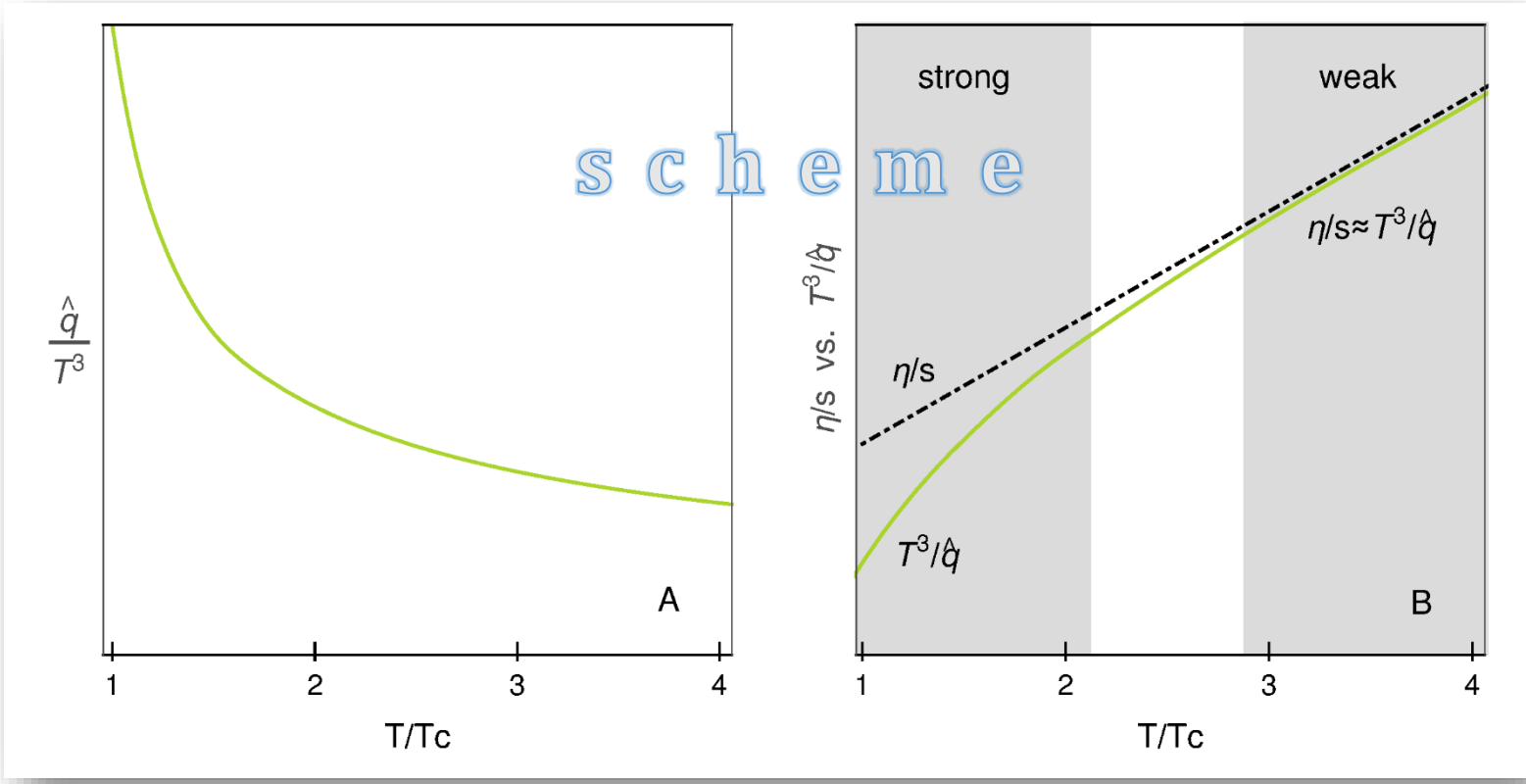

s c h e m e

B. Karmakar, D. Zigic, I. Salom, J. Auvinen, P. Huovinen, M. Djordjevic and MD, PRC **108**, 044907 (2023).

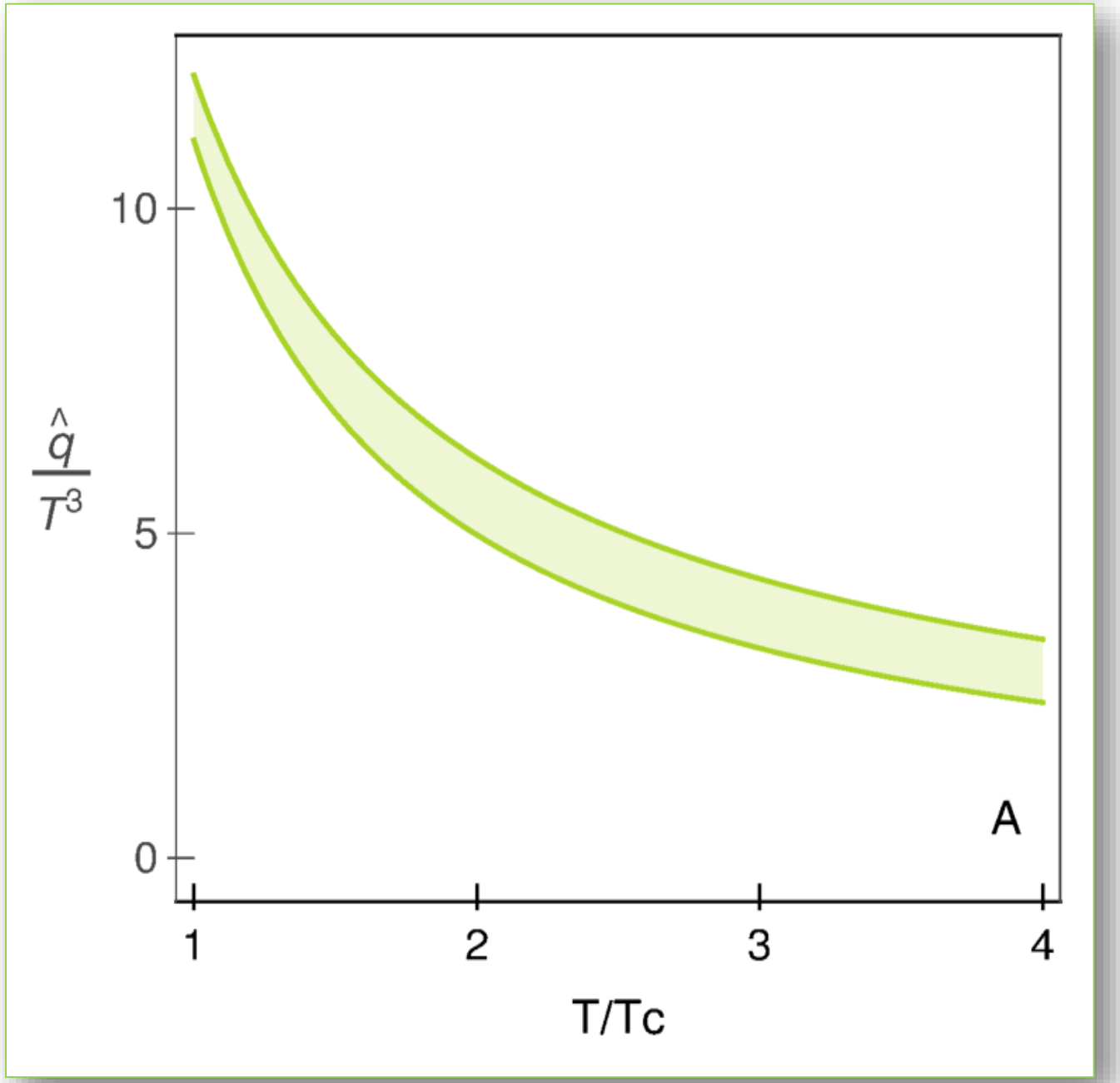

B. Karmakar, D. Zigic, I. Salom, J. Auvinen, P. Huovinen, M. Djordjevic and MD, PRC **108**, 044907 (2023).

$\frac{\hat{q}}{T^3}$ shows expected behavior, i.e., enhanced quenching near *Tc*.

The enhancement arises from chromo-electric and chromo-magnetic interplay, absent in static models, underscoring dynamic medium importance in energy loss calculations.

Comparison with Bayesian analyses and Summary of Part I

Blue: Nature Phys. 15,no. 11,1113-1117(2019)

Gray: Phys. Rev. C 102,044911 (2020)

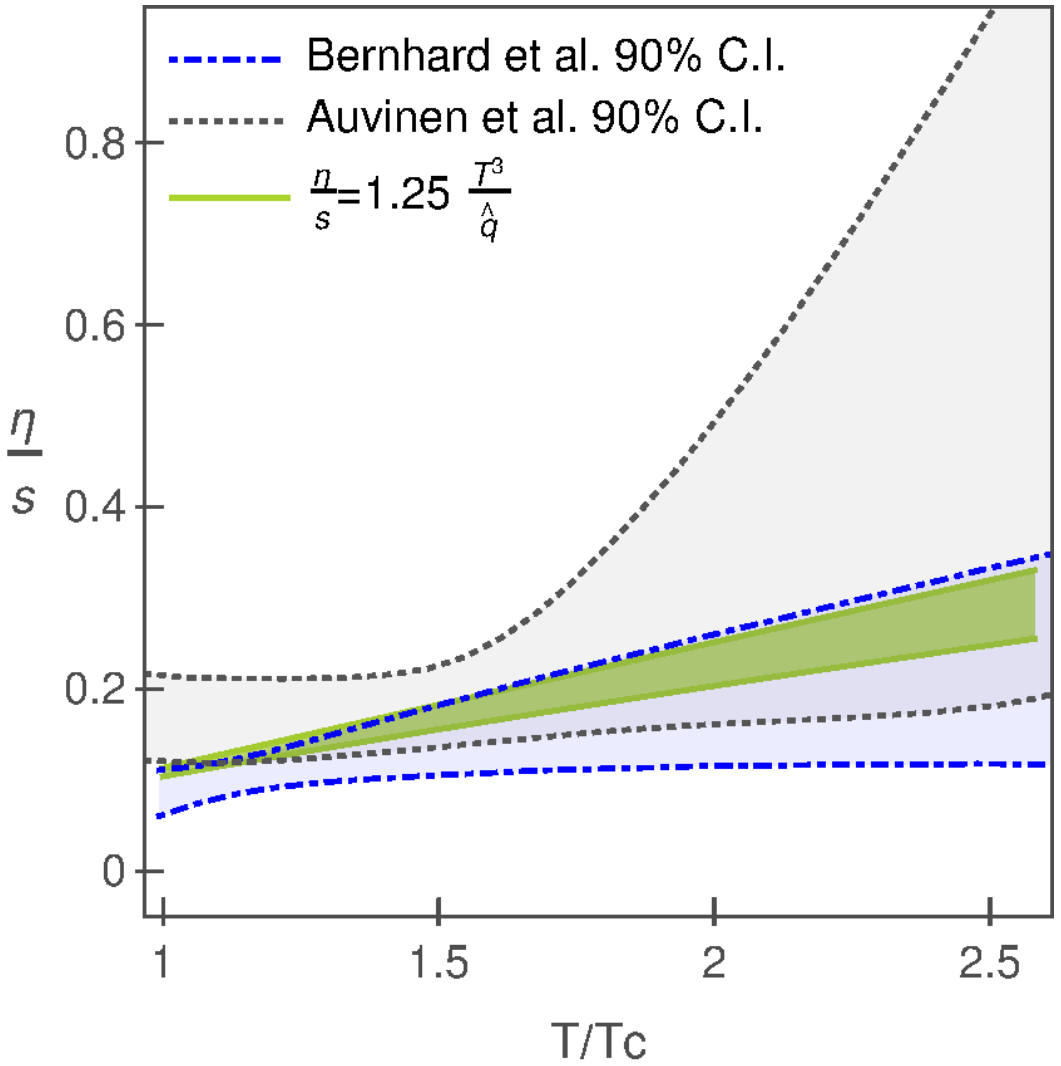

- η/s shows surprisingly good agreement all the way to T_c with constraints extracted from existing Bayesian analyses. (i.e., it falls precisely in the overlap of the two intervals).
- This agreement is surprising, as near T_c we expect divergence due to strong coupling.
- While the extended agreement supports our dynamical energy loss model's predictive ability, it raises a question about the absence of expected behavior.
- It is unlikely that the weak coupling regime would extend down to Tc.
- Instead, it was proposed that $\eta/s \approx 1.25\frac{T^3}{\hat{q}}$ holds as long as the quasiparticle picture of QGP is applicable., a condition also necessary for the accuracy of energy loss calculations, such as our dynamical model.
- **Intriguing hypothesis:** The quasiparticle picture remains valid at the entire temperature range.
- This obscures estimation of the soft-to-hard boundary, a major unresolved issue.

B. Karmakar, D. Zigic, I. Salom, J. Auvinen, P. Huovinen, M. Djordjevic and MD, PRC **108**, 044907 (2023).

Part II: Inferring bulk QGP properties

Bulk QGP properties are traditionally explored by low-pt observables that describe the collective motion of 99.9% of QCD matter.

Rare high energy probes are, on the other hand, almost exclusively used to understand high-pt parton - medium interactions.

However, some important bulk QGP properties are known to be difficult to constrain by low-pt observables and corresponding theory/simulations.

While high-pt physics had a decisive role in QGP discovery, it has been rarely used to understand bulk QGP properties.

We advocate high-pt QGP tomography, where low- and high-pt physics jointly constrain bulk QGP parameters.

European Research Council

The main idea behind the QGP tomography

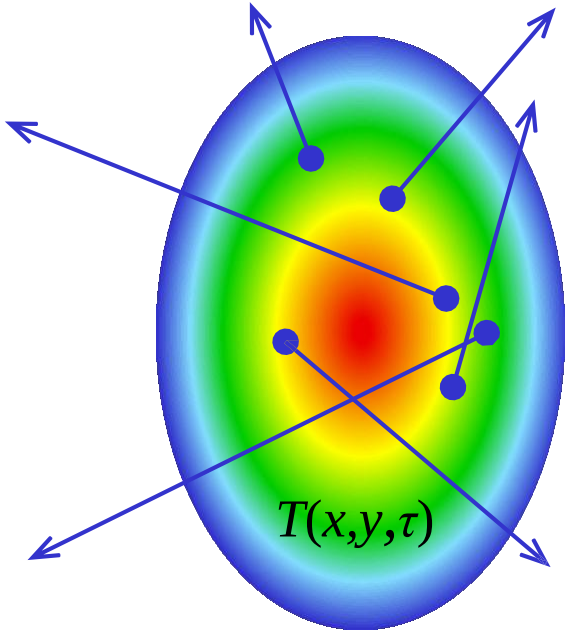

When high-pt particles go through QGP, they lose energy.

This energy loss depends on the temperature evolution of the QGP.

Temperature evolutions are different for different QGP parameters

This energy loss is sensitive to QGP properties.

We can realistically predict this energy loss.

High-pt probes are powerful tomographic tools.

Use them to infer some bulk QGP properties.

DREENA-A framework as a QGP tomography tool

To use high pt data/theory to explore the bulk QGP:

- Include any, arbitrary, medium evolution as an input.
- Preserve all dynamical energy loss model properties.
- Develop an efficient (timewise) numerical procedure.
- Generate a comprehensive set of light and heavy flavor predictions.
- Compare predictions with the available experimental data.
- If needed, iterate a comparison for different combinations of QGP medium parameters.
- Extract medium properties consistent with both low and high-pt theory and data.

Develop fully optimized DREENA-A framework.

DREENA: Dynamical Radiative and Elastic ENergy loss Approach; A: Adaptive temperature profile.

D.Zigic, I.Salom, J.Auvinen, P.Huovinen, M. Djordjevic Front.in Phys. 10(2022)957019

Optimized to incorporate any arbitrary event-by-event fluctuating temperature profile.

D.Zigic, J.Auvinen, I.Salom, M. Djordjevic, P.Huovinen Phys.Rev.C 106(2022)4, 044909

DREENA-A is available on http://github.com/DusanZigic/DREENA-A

Qualitative differences between T profiles

All three evolutions agree with low-pt data. Can high pt-data provide further constraint?

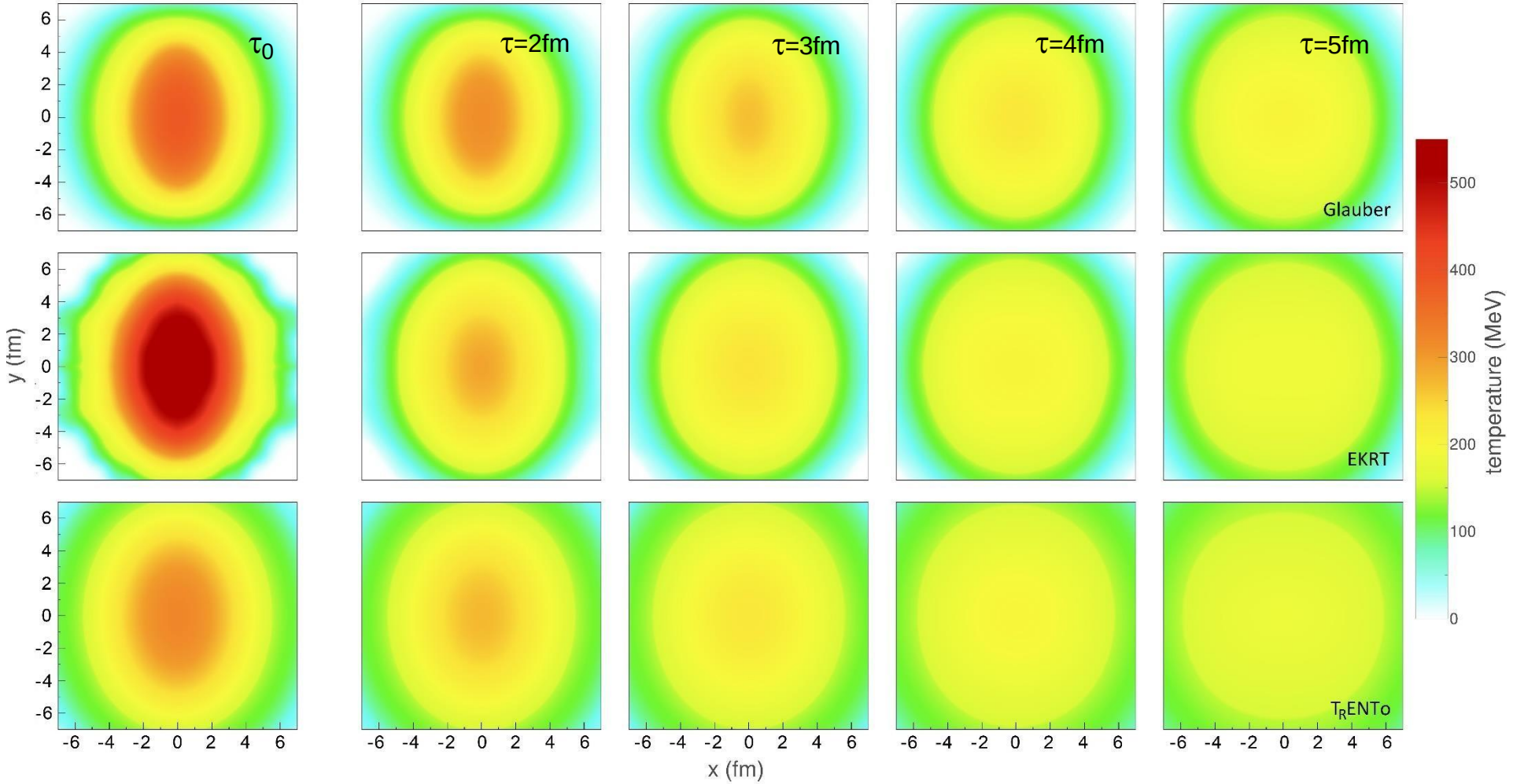

- Largest anisotropy for Glauber (τ_0=1fm) – expected differences in high-pt v_2.
- EKRT shows larger temperature - smaller R_{AA} expected.

DREENA-A predictions

D. Zigic, I. Salom, J. Auvinen, P. Huovinen and MD, Front.in Phys. 10 (2022) 957019

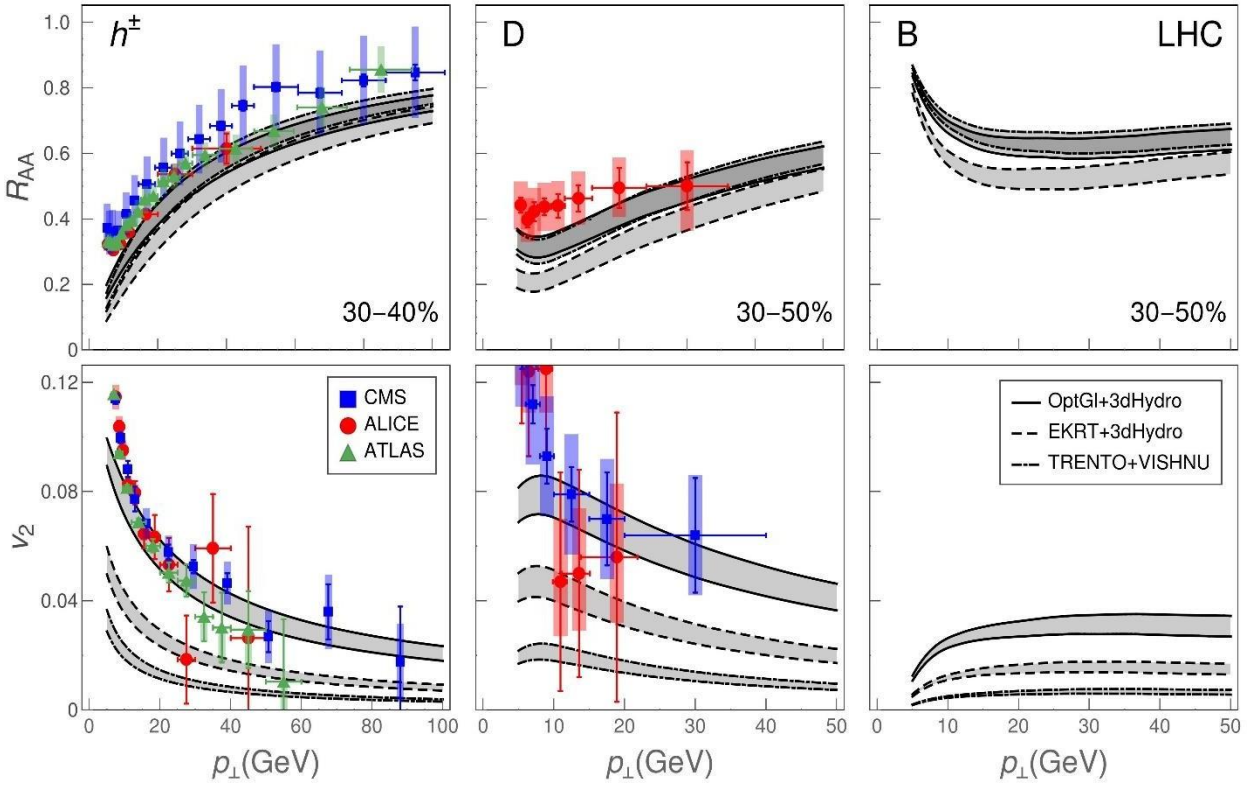

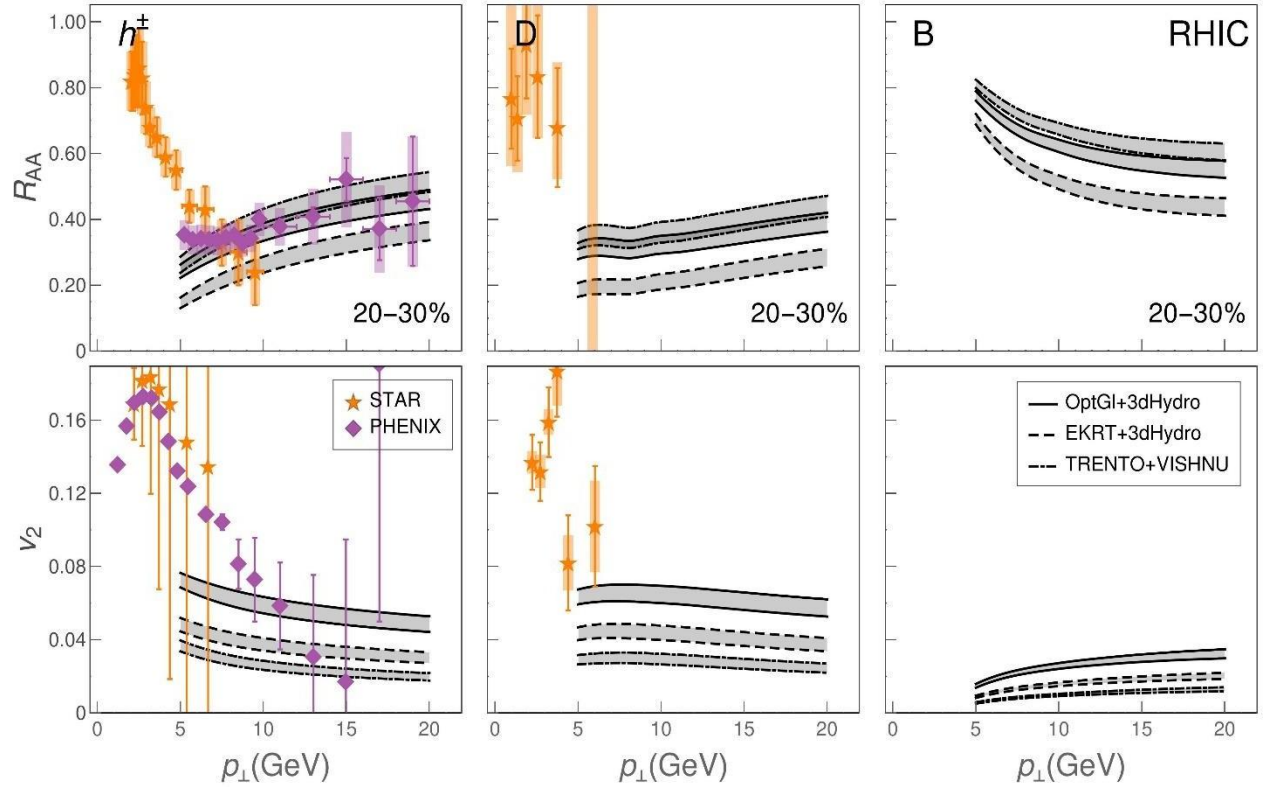

- 'EKRT' indeed leads to the smallest R_{AA}.
- Anisotropy translates to v_2 differences ('Glauber' largest, T$_R$ENTo lowest).
  - DREENA-A can differentiate between different *T* profiles.
    - Additional (independent) constraint to low-pt data.

Importance of higher harmonics for QGP tomography

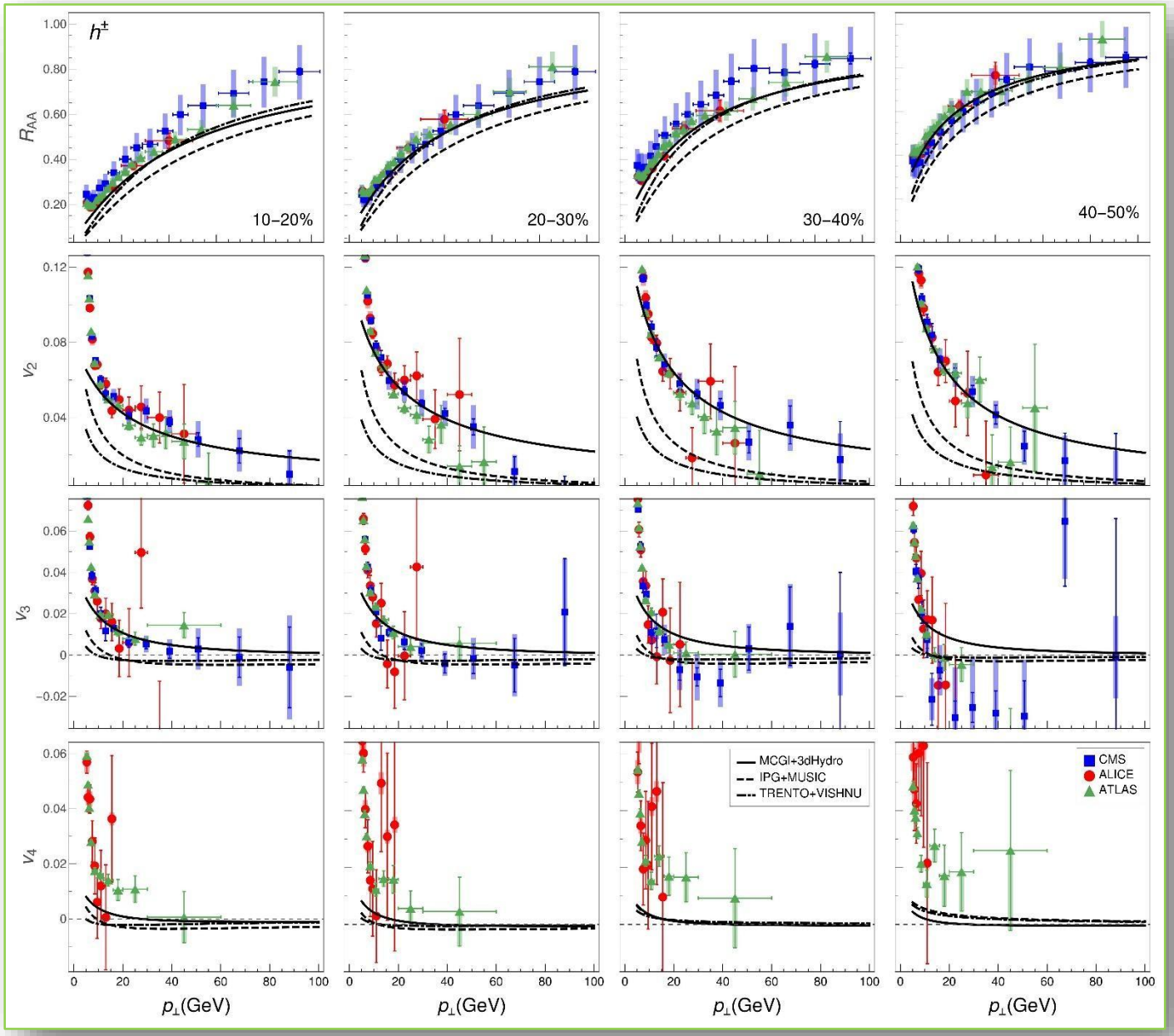

D. Zigic, J. Auvinen, I. Salom, P. Huovinen and MD, Phys.Rev.C 106 (2022) 4, 044909

- High-pt data are available up to the 7^{th} harmonic (for ATLAS) and cover the pt region up to 100 GeV (for CMS).
- State of the art in the experimental sector, but theoretically not well explored!
- **Can higher harmonics be used for precision QGP tomography?**

- Higher harmonics can both qualitatively and quantitatively distinguish between different medium evolutions!
- Existent v_4 data are far above all model predictions – a possible v_4 puzzle!

Heavy flavor higher harmonics

D. Zigic, J. Auvinen, I. Salom, P. Huovinen and MD, Phys.Rev.C 106 (2022) 4, 044909

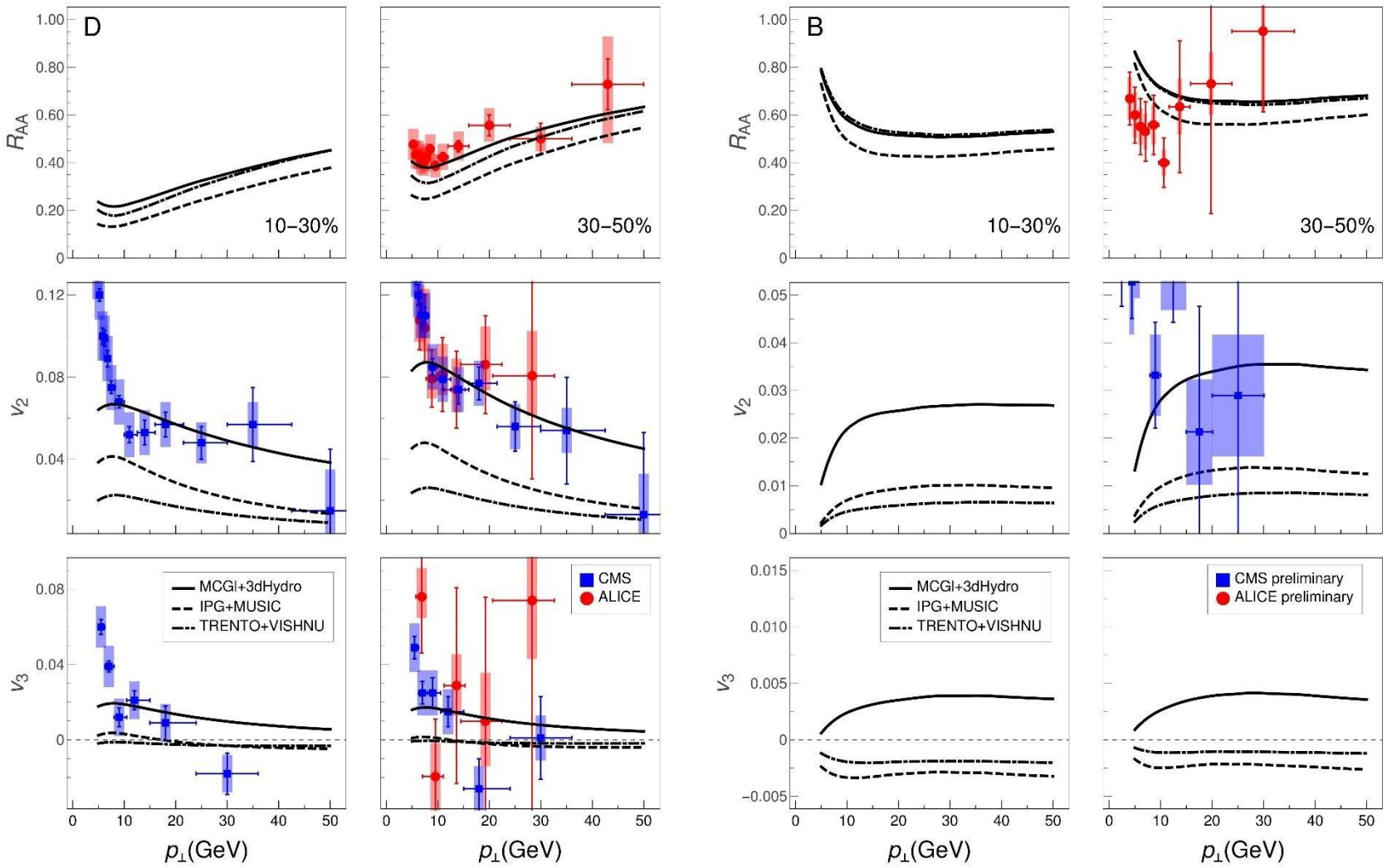

- Heavy flavor - even more sensitive to different medium evolutions!
- Upcoming high-luminosity data at RHIC and LHC will provide higher harmonics data with much larger precision.
- Higher harmonics present a unique opportunity for precision QGP tomography.
- Adequate medium evolution should be able to all experimental data simultaneously, for both light and heavy flavor, at different centralities and collision energies.

Exploring bulk QGP properties through DREENA

Constrained the early evolution of QGP.

S. Stojku., J. Auvinen, M. Djordjevic, P. Huovinen and MD, Phys. Rev. C Lett. **105**, L021901 (2022).

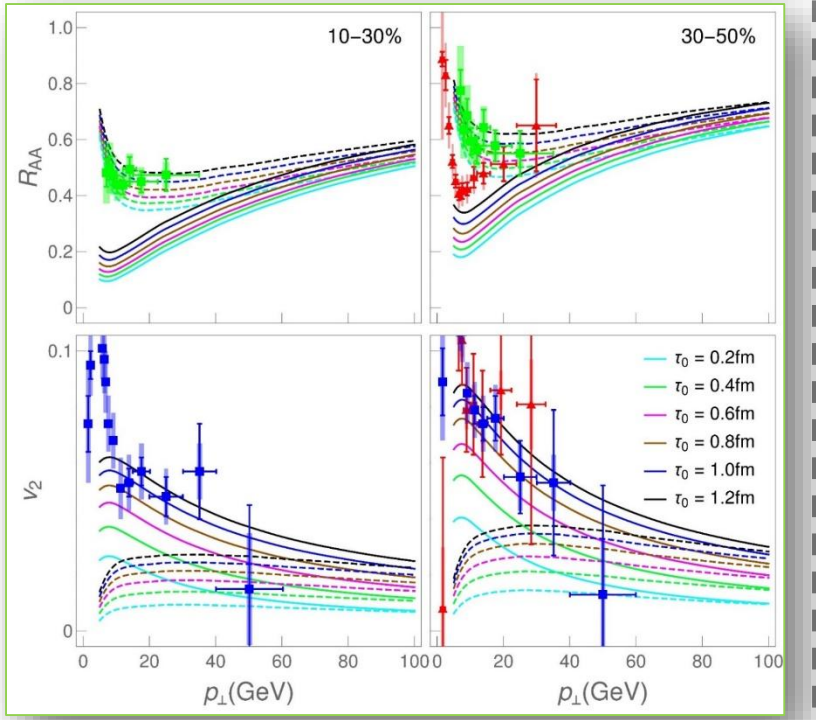

Proposed a new observable to constrain QGP anisotropy

S. Stojku, J. Auvinen, L. Zivkovic, P. Huovinen, MD, Physics Letters B **835**, 137501 (2022).

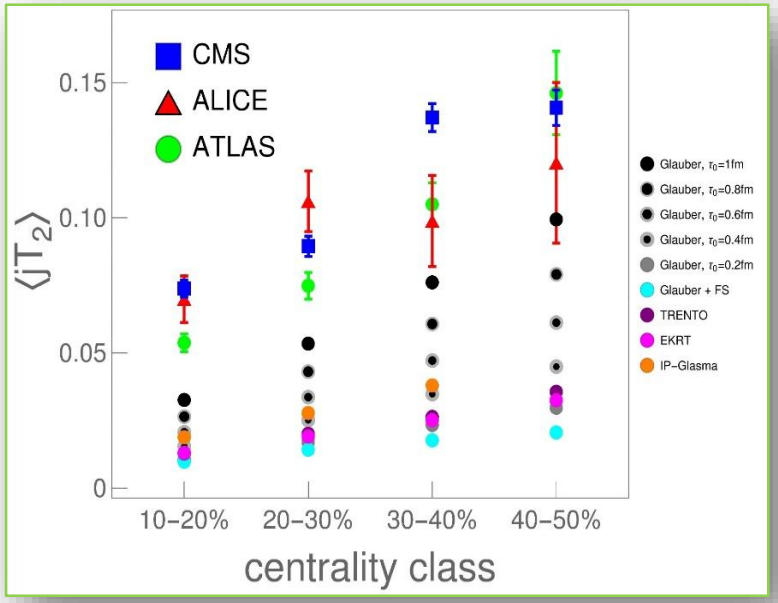

Probed the shape of the QGP droplet with ebeDREENA

B. Karmakar, D. Zigic, P. Huovinen, M. Djordjevic, MD, and J. Auvinen, arXiv: Phys. Rev. C **110**, 044906 (2024).

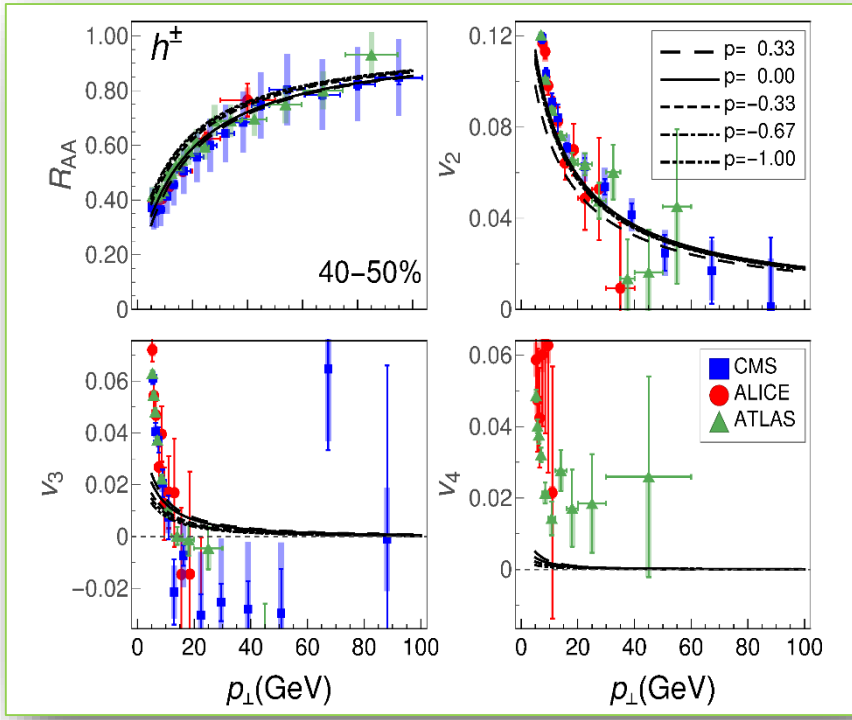

What next?

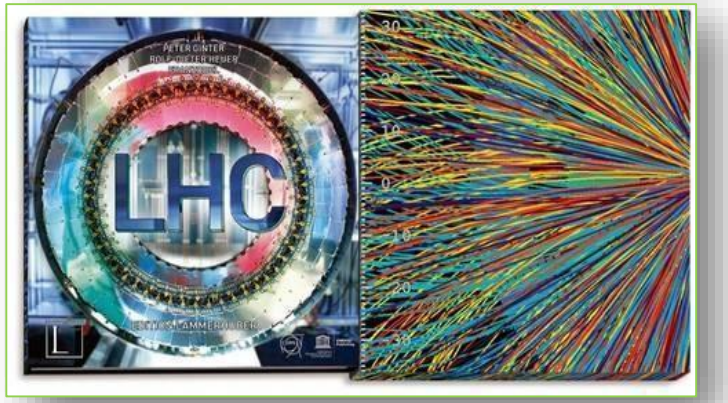

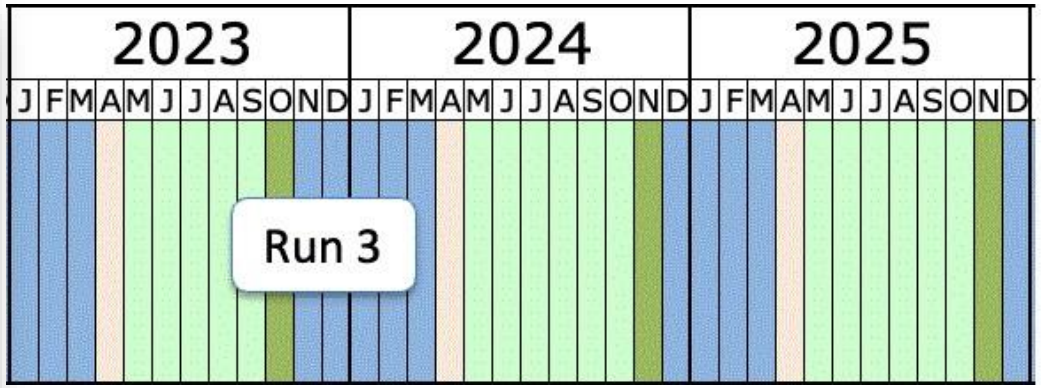

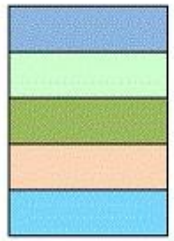

Shutdown/Technical stop
Protons physics
Ions
Commissioning with beam
Hardware commissioning

sPHENIX

2023	2024	2024	2025
Au+Au	p-p	p+Au	Au+Au
Calibration	Ref. measurements for HI		High statistics

Ongoing high-precision era at RHIC and LHC

DREENA can enable better utilization of these large scientific investments, as well as precise determination of the properties of this extreme state of matter.

Formal framework for DREENA Bayesian inference

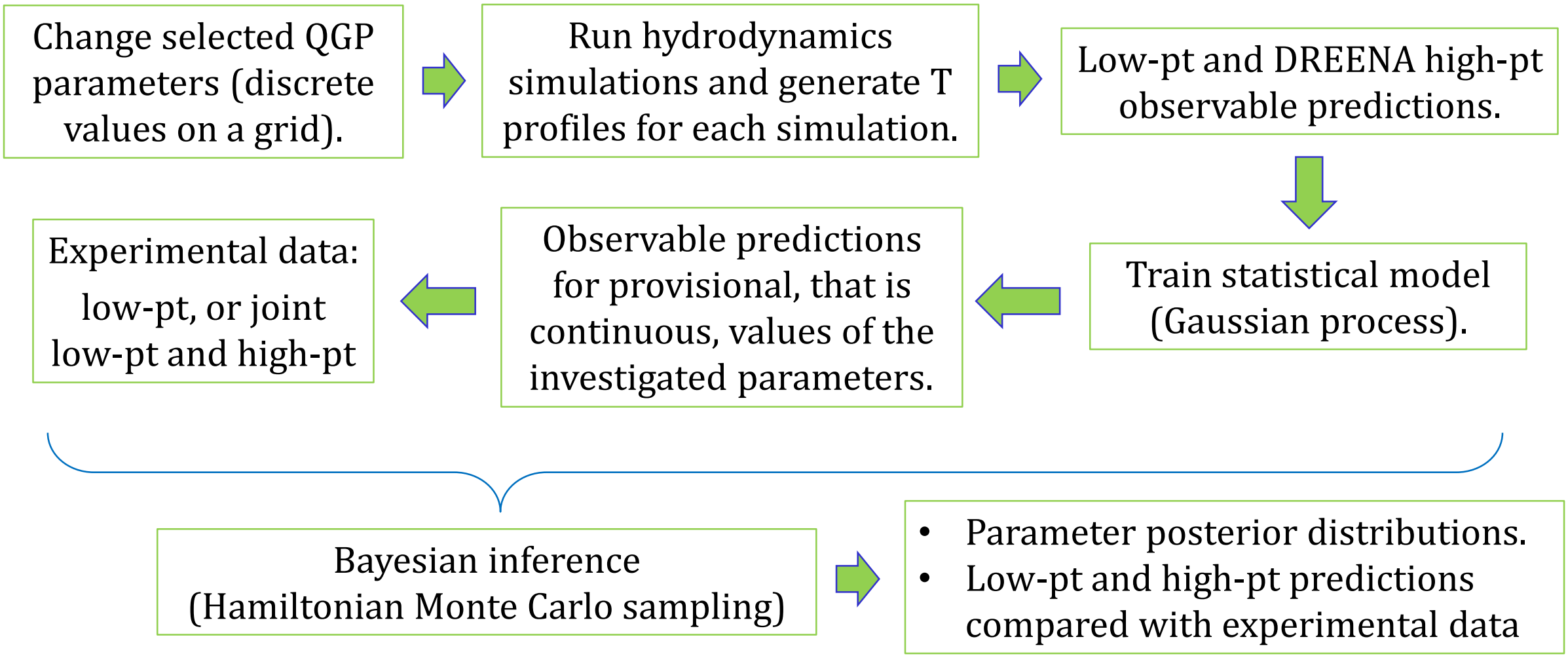

- Weassume TRENTo with p=0, and run (2+1)-dimensional fluid dynamical model (VISHNU) with no free streaming.
- Generated latin hypercube with 200 points, with norm, τ and η/s in the following ranges:
  - τ: 0.2-1.3 fm
  - Constant η/s: 0.02-0.2
  - Norm: 60-360

  All other parameters are as in PRC **108**, 044907 (2023).
- For each set of parameters, we run average medium evolutions with TRENTo+ VISHNU, to generate low-pt predictions and *T* profiles as an input for DREENA-A.
- Run DREENA-A with these *T* profiles to generate high-pt predictions.
- Statistical inference framework (previous slide) is then employed with these predictions either on only low-pt experimatal data, or jointly on low-pt and high-pt experimental data.

Marginal distribution of parameters obtained with Bayesian inference of low-pt data

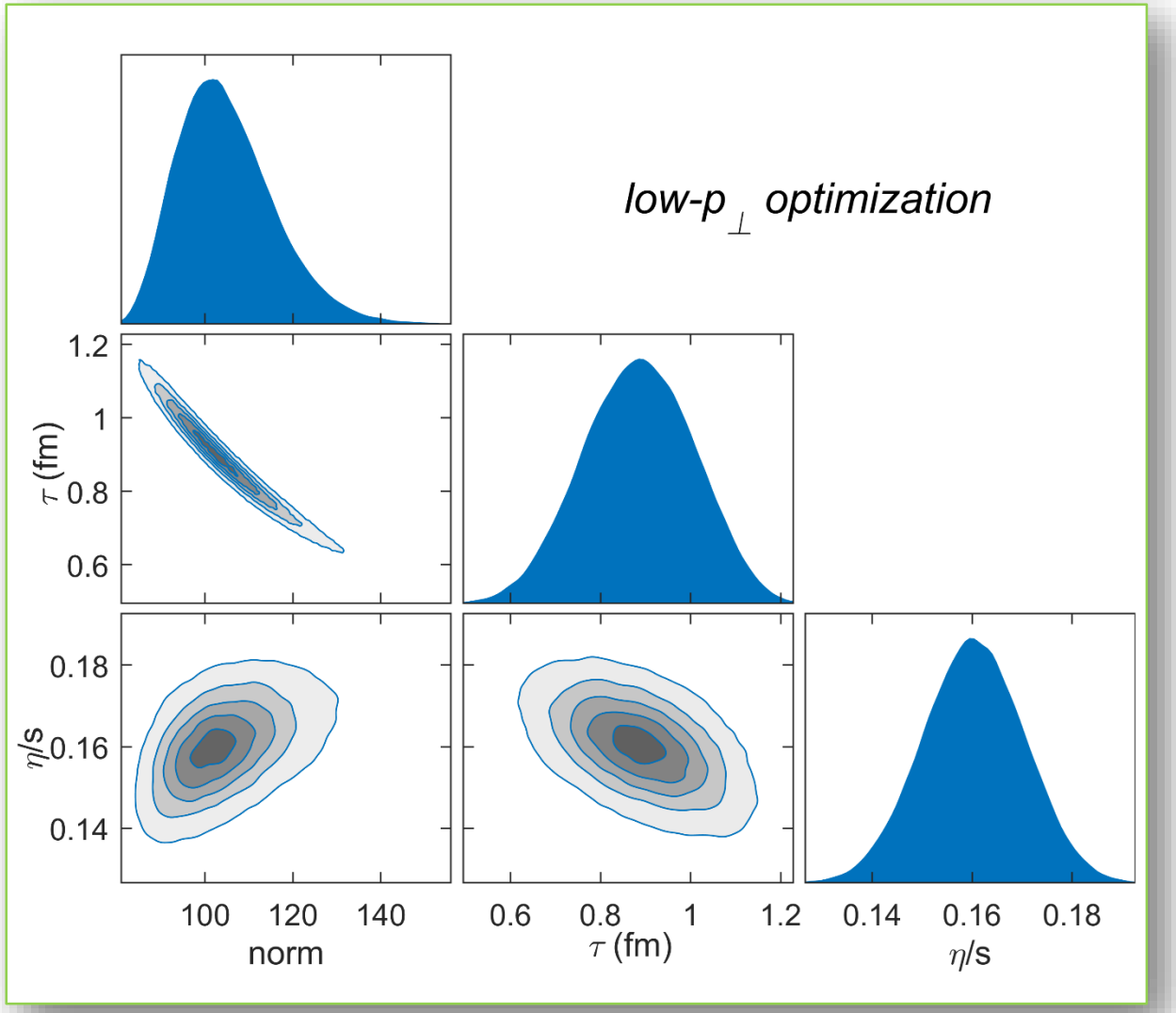

M. Djordjevic, D. Zigic, I. Salom, and MD, arXiv:2603.09584

Prior vs. posterior

low-pt data

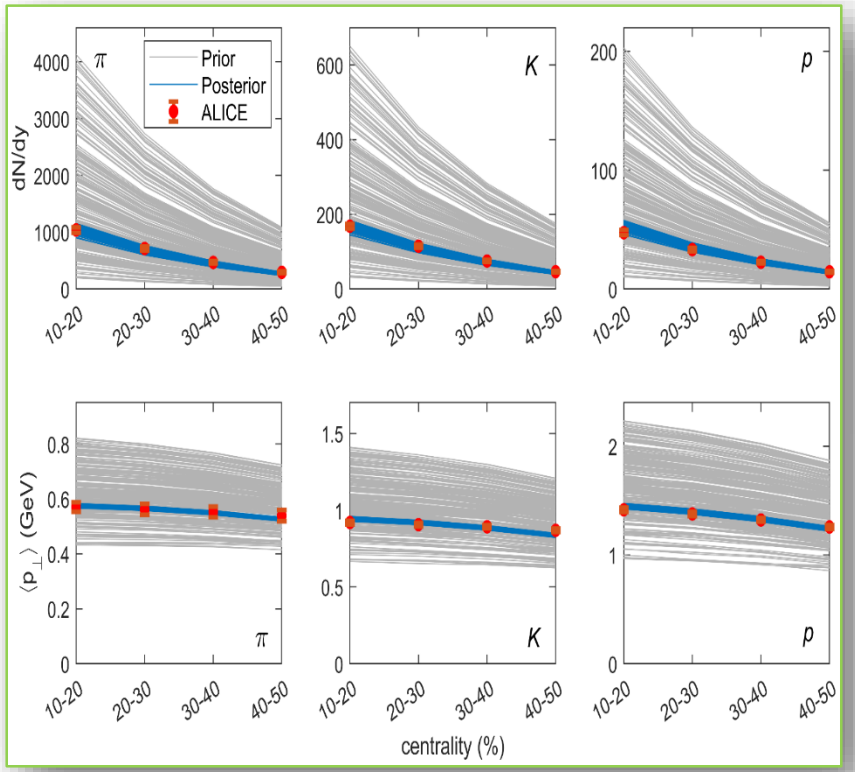

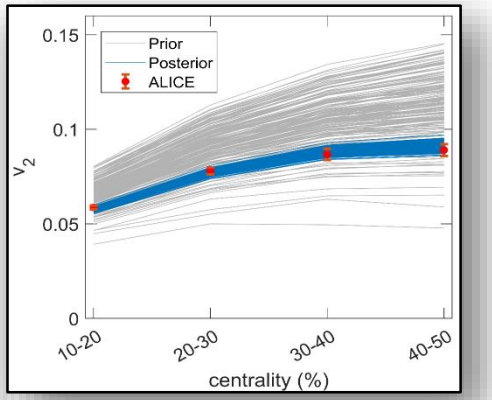

Very good agreement with low-pt data!

M. Djordjevic, D. Zigic, I. Salom, and MD, arXiv:2603.09584

high-pt data

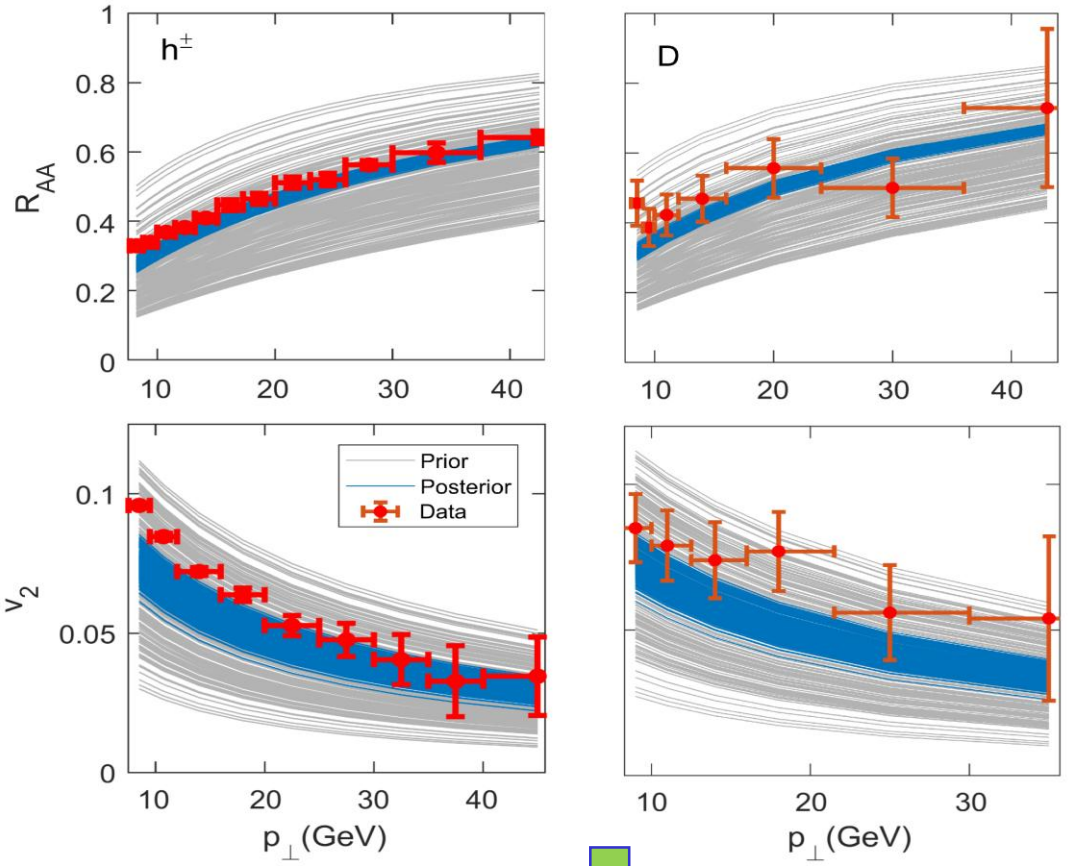

Suboptimal agreement with high-pt data, especially for v_2.

Marginal distribution of parameters obtained with Bayesian inference of both low-pt and high-pt data

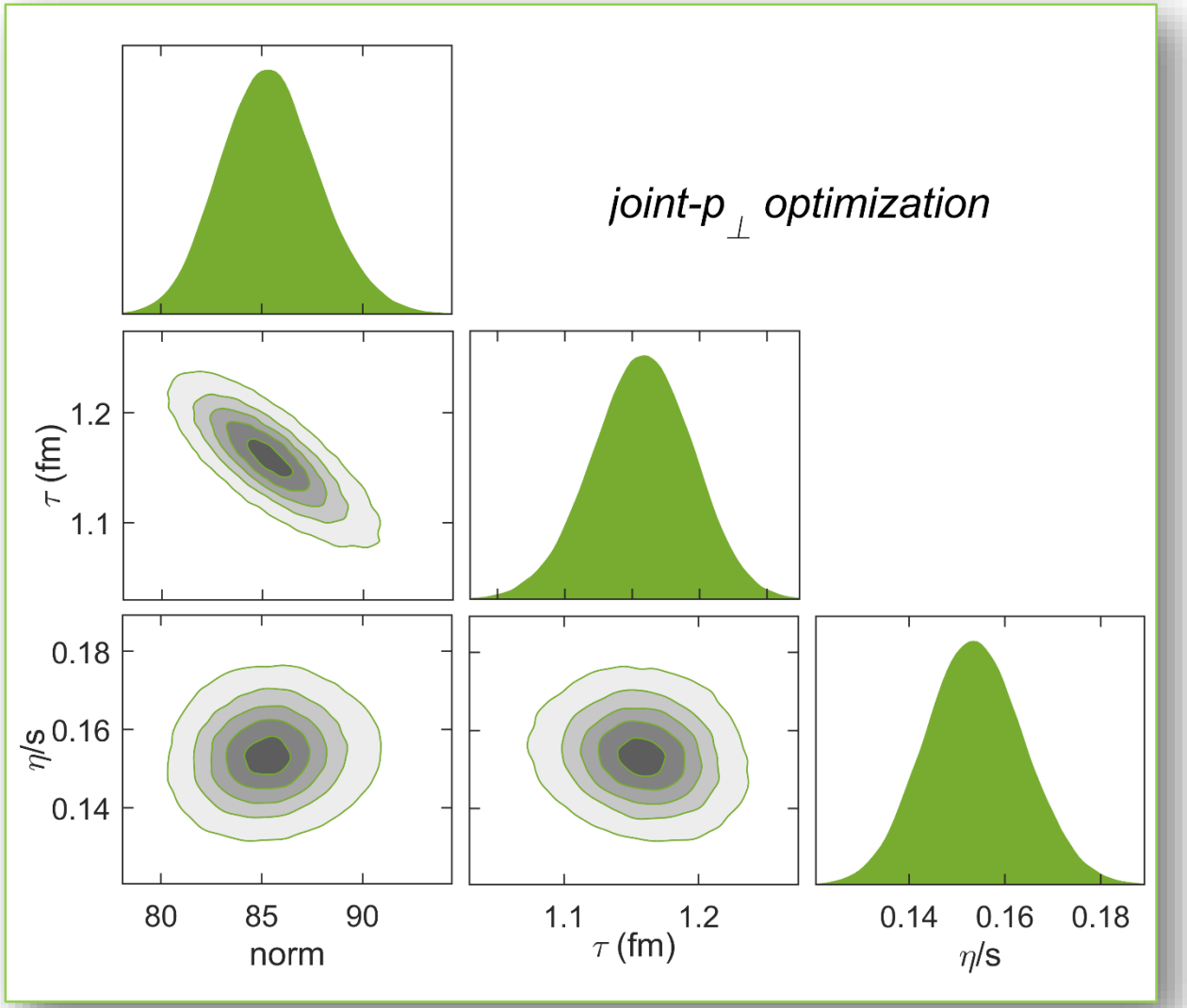

M. Djordjevic, D. Zigic, I. Salom, and MD, arXiv:2603.09584

Prior vs. posterior

low-pt data

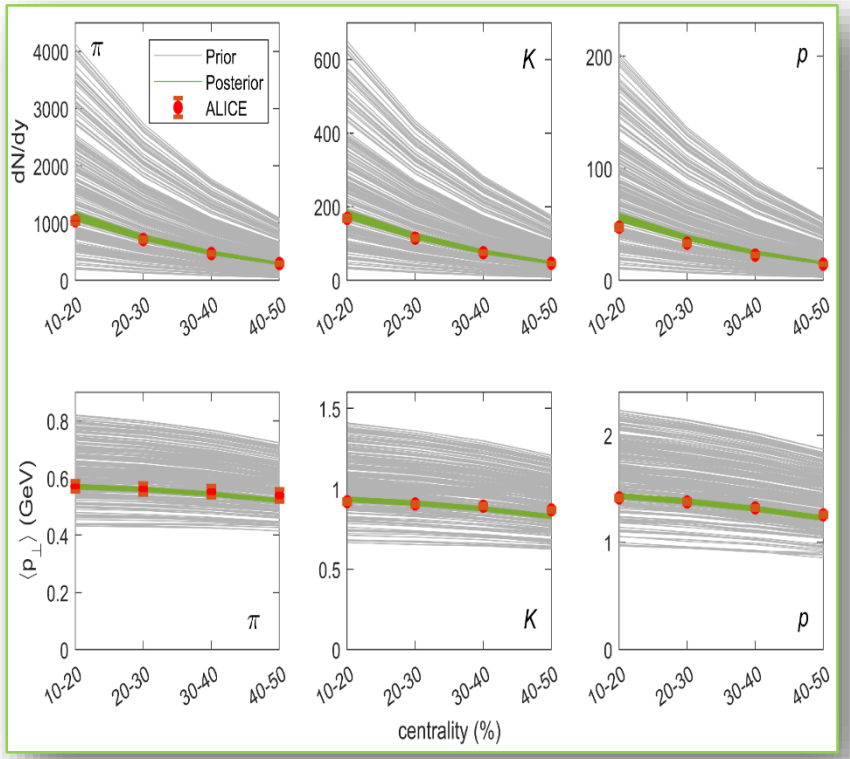

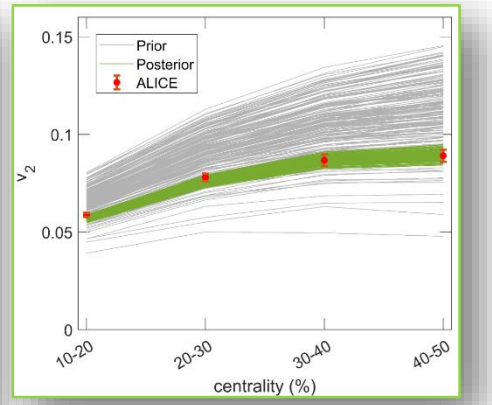

Very good agreement with low-pt data!

M. Djordjevic, D. Zigic, I. Salom, and MD, arXiv:2603.09584

high-pt data

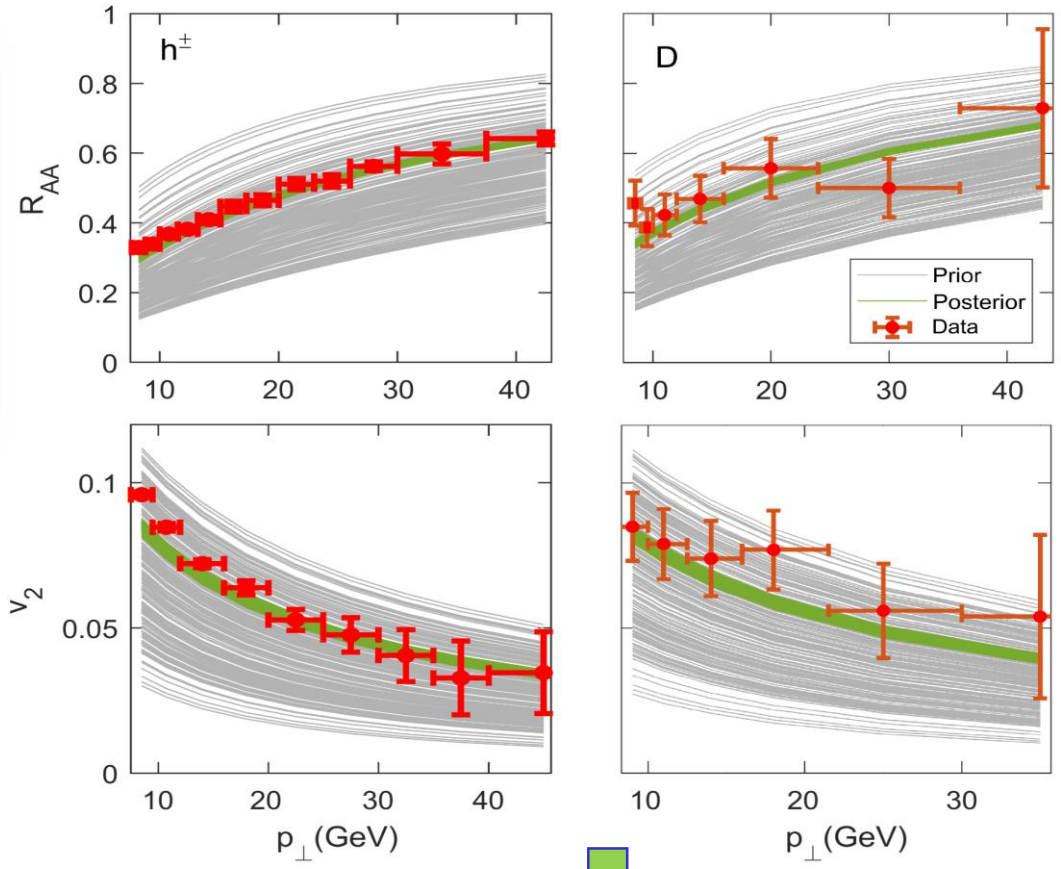

Very good agreement with high-pt data as well!

Comparison of marginal parameter distributions from low-pt-only and joint low-/high-pt Bayesian inference

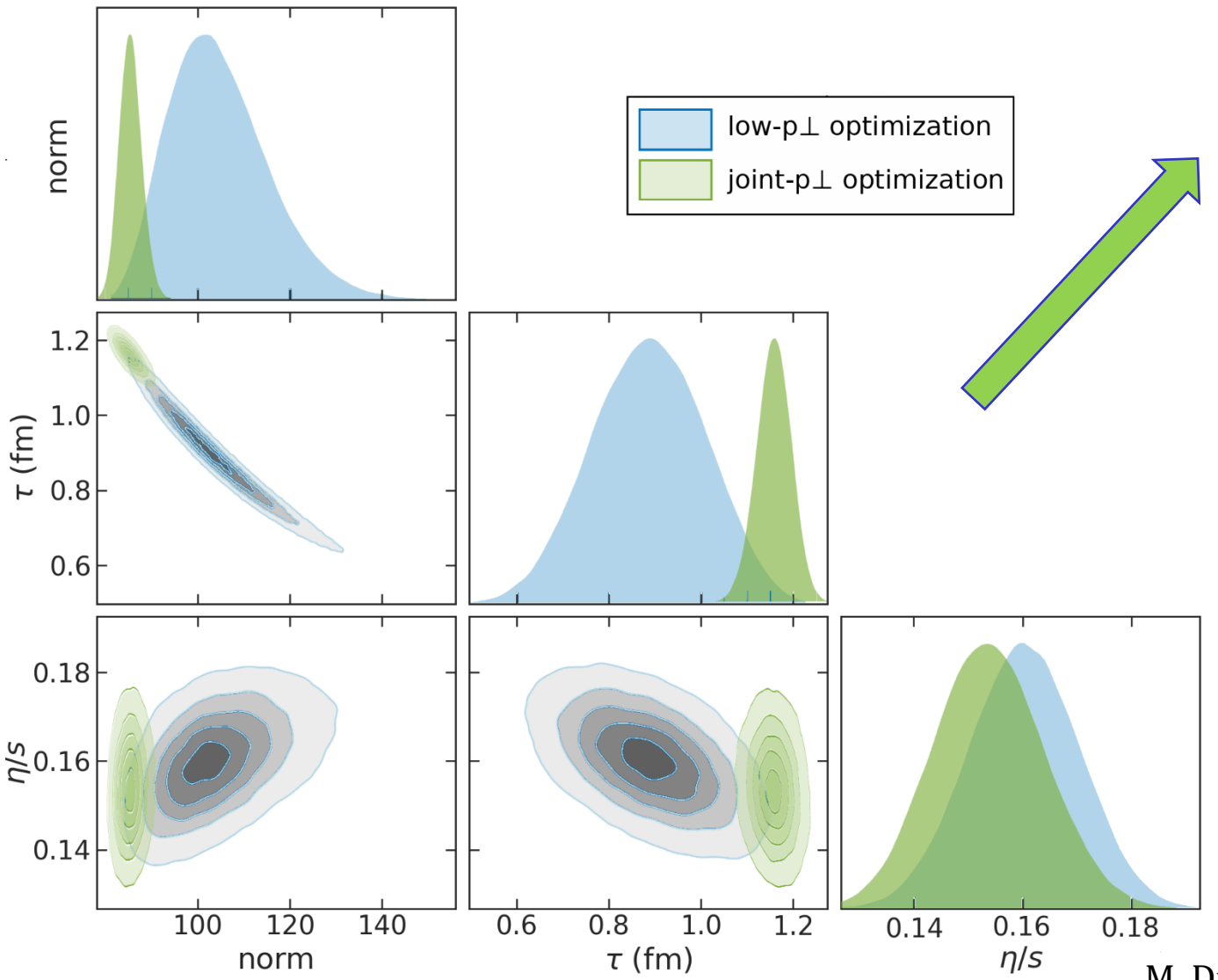

Distributions are not inconsistent with each other!

Inclusion of high-pt data significantly narrows the distributions of parameters!

High-pt data are necessary for precision extraction of bulk QGP parameters!

Overall, jet tomography is crucial for constraining QGP properties!

M. Djordjevic, D. Zigic, I. Salom, and MD, arXiv:2603.09584

Summary: Optimizing QGP Parameter Extraction

- Unifying low-pt and high-pt theory and data with advanced Bayesian statistics significantly improves constraints on QGP properties. High-pt data from RHIC and LHC were underutilized for this purpose, and this approach enables their optimal use.

What do we need from the experimental data at the LHC and RHIC in the high-precision era to optimally extract QGP parameters?

- Improved agreement between different experiments within the LHC.
  - Precise extraction of QGP parameters is challenging if the data from different experiments agree within large error bars.
- Precise measurements for high-pt D meson R_{AA}, v_2, and higher harmonics.
- Precise measurements for at least B meson high-pt R_{AA} and v_2 data.
  - Due to the dead cone effect, B mesons provide an independent variable, offering a much better constraint on QGP parameters. Models must simultaneously explain both low and high-pt data, and within high-pt data, they need to account for both light and heavy flavor.
- Precise measurements for inclusive jet R_{AA} and v_2 data for several R.

From partons to jets: extending dynamical radiative energy loss

$$\frac{d^2N_g^{\rm rad}}{dx\,d\tau} = \int \frac{d^2k}{\pi}\frac{d^2q}{\pi}\,\frac{2\,C_R C_2(G)\,T}{x}\,\frac{\alpha_S(ET)\,\alpha_S\!\left(\frac{k^2+\chi(T)}{x}\right)}{\pi}\,\frac{\mu_E^2(T)-\mu_M^2(T)}{(q^2+\mu_M^2(T))(q^2+\mu_E^2(T))}$$
$$\times\frac{(k+q)}{(k+q)^2+\chi(T)}\left[\frac{(k+q)}{(k+q)^2+\chi(T)}-\frac{k}{k^2+\chi(T)}\right]\left(1-\cos\left[\frac{(k+q)^2+\chi(T)}{xE^+}\,\tau\right]\right)\Theta\left(\frac{|k|}{xE}-R\right).$$

We generalized a 1st order opacity, HTL-based radiative kernel to include space-time-dependent temperature evolution and the jet radius *R*.

- Applies to single partons (R=0) and jets (R>0) through an out-of-cone selection.
- The same microscopic framework both partons and jets, applicable for both light and heavy flavor.

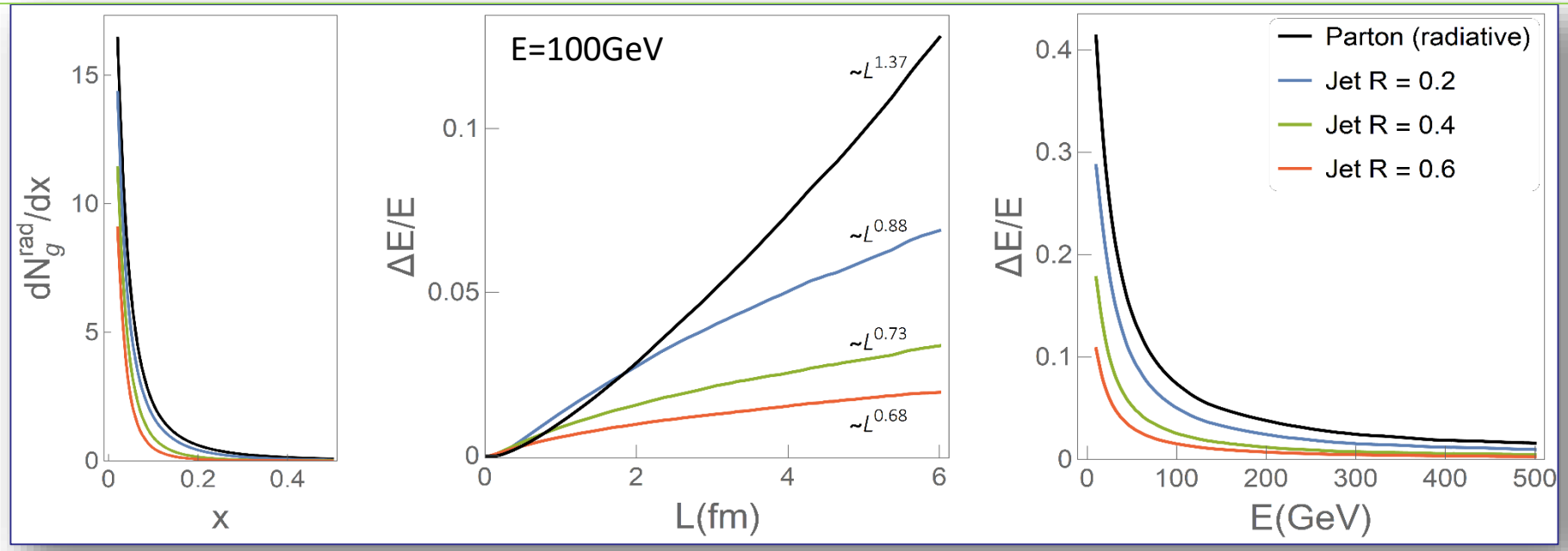

B. Karmakar, MD, arXiv:2412.17106

Effective path-length scaling weakens for jets
The jet exponents become clearly **sublinear**, and decrease further with increasing *R*.

Increasing the cone radius suppresses out-of-cone radiation.
The jet curves lie progressively below the parton result as more radiation is kept inside the cone.

Cone-dependent collisional energy loss

$$\Delta E_{el}^{(R)} = \int_0^\infty n_{eq}(|\vec{\mathbf{k}}|)d|\vec{\mathbf{k}}| \left(\int_0^{|\vec{\mathbf{k}}|} |\vec{\mathbf{q}}|d|\vec{\mathbf{q}}| \int_{-|\vec{\mathbf{q}}|}^{|\vec{\mathbf{q}}|} \omega d\omega + \int_{|\vec{\mathbf{k}}|}^{|\vec{\mathbf{q}}|_{max}} |\vec{\mathbf{q}}|d|\vec{\mathbf{q}}| \int_{|\vec{\mathbf{q}}|-2|\vec{\mathbf{k}}|}^{|\vec{\mathbf{q}}|} \omega d\omega \right) \frac{8\,C_R}{\pi^2}\, \alpha_S(ET)\, \alpha_S(\mu_E^2)$$

$$\left\{ |\Delta_L(q)|^2 \frac{(2|\vec{\mathbf{k}}|+\omega)^2 - |\vec{\mathbf{q}}|^2}{2} \mathcal{J}_1^{(R)} + |\Delta_T(q)|^2 \frac{(|\vec{\mathbf{q}}|^2-\omega^2)[(2|\vec{\mathbf{k}}|+\omega)^2+|\vec{\mathbf{q}}|^2]}{4|\vec{\mathbf{q}}|^4} \left[(v^2|\vec{\mathbf{q}}|^2-\omega^2)\mathcal{J}_1^{(R)} + 2\omega\mathcal{J}_2^{(R)} - \mathcal{J}_3^{(R)} \right] \right.$$

We generalized finite-size, finite T HTL-based collisional kernel to include jet radius *R*:

- Keeps track of what leaves the cone.
- Separates the primary jet contribution from the recoil sector, allowing a clean estimate of the medium response effect.
- Applicable to both light and heavy flavor.
- R→0 reproduces the partonic elastic loss, R→π gives complete in-cone recovery.

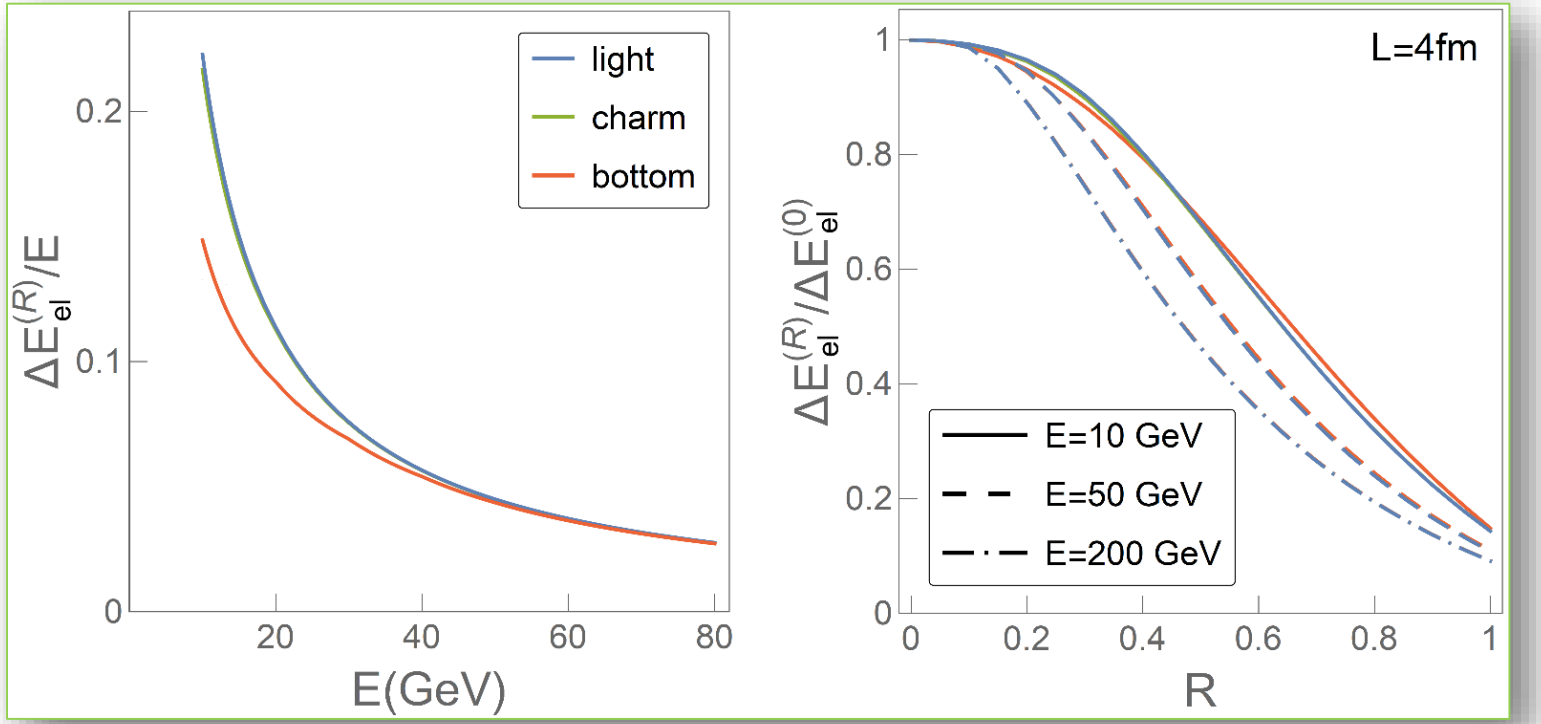

MD, B. Ilic, M. Djordjevic, arXiv:2601.21655

What changes for jets?

MD, B. Ilić, M. Djordjevic, arXiv:2601.21655

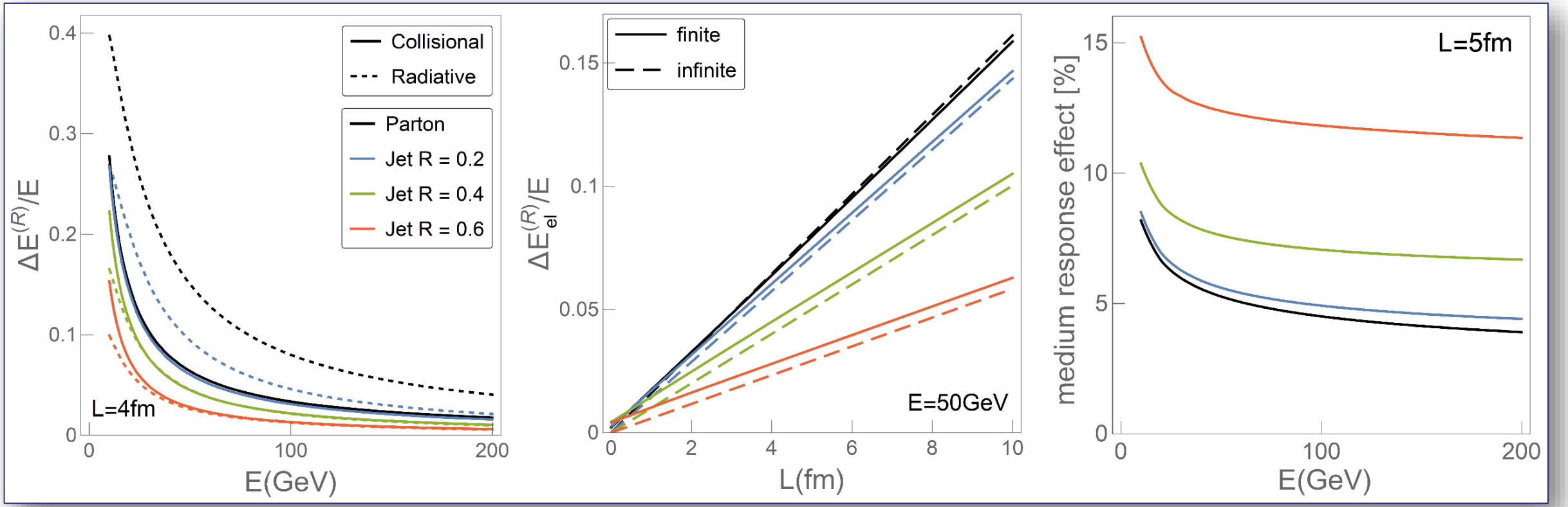

At ***R* = 0** the usual hierarchy is recovered: **radiative > collisional**

Radiative loss strongly decreases with increasing R, while the collisional component decreases more slowly and **exceeds radiative for larger R.**

Elastic path-length dependence stays close to **linear**, and finite-size corrections remain modest.

The medium respose effect is only a few percent for partons, but exceeds 10% for realistic jet radii.

Next step: These results provide the missing ingredients needed to extend DREENA from hadrons to jets, and to enable future Bayesian inference within a fully dynamical jet-capable framework.

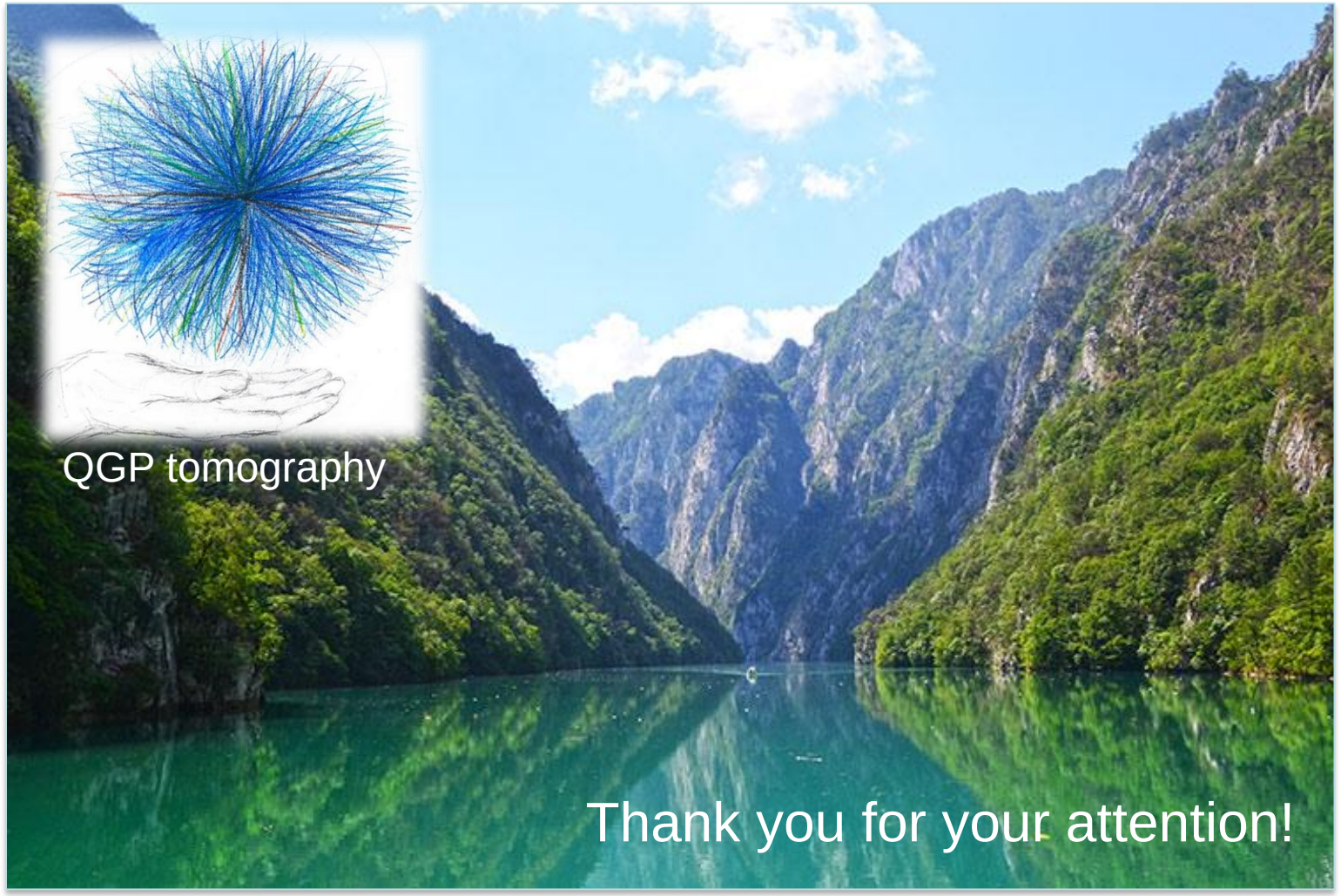

Canyon of river DREENA in Serbia

European Research Council
Established by the European Commission

МИНИСТАРСТВО ПРОСВЕТЕ,
НАУКЕ И ТЕХНОЛОШКОГ РАЗВОЈА

Backup

A. Modeling the bulk evolution

- Initial entropy profiles are generated using TRENTo model.
- 10^4 events for Pb+Pb (5.02 TeV) and Au+Au (200 GeV).
- Events sorted in centrality classes.
- Initial free streaming is not preferred by high-$p_\perp$ data.
  S. Stojku, J. Auvinen, M. Djordjevic, P. Huovinen and MD, Phys. Rev. C 105 (2022) 2, L021901
- Onset time for hydrodynamics: $\tau_0 = 1 fm$.
  S. Stojku, J. Auvinen, M. Djordjevic, P. Huovinen and MD, Phys. Rev. C 105 (2022) 2, L021901
- (2+1)-dimensional fluid dynamical model (VISHNew) used to simulate the medium evolution.

B. Karmakar, D. Zigic, I. Salom, J. Auvinen, P. Huovinen, M. Djordjevic and MD, PRC **108**, 044907 (2023).

Radiative jet energy loss: path-length dependence in expanding vs static medium

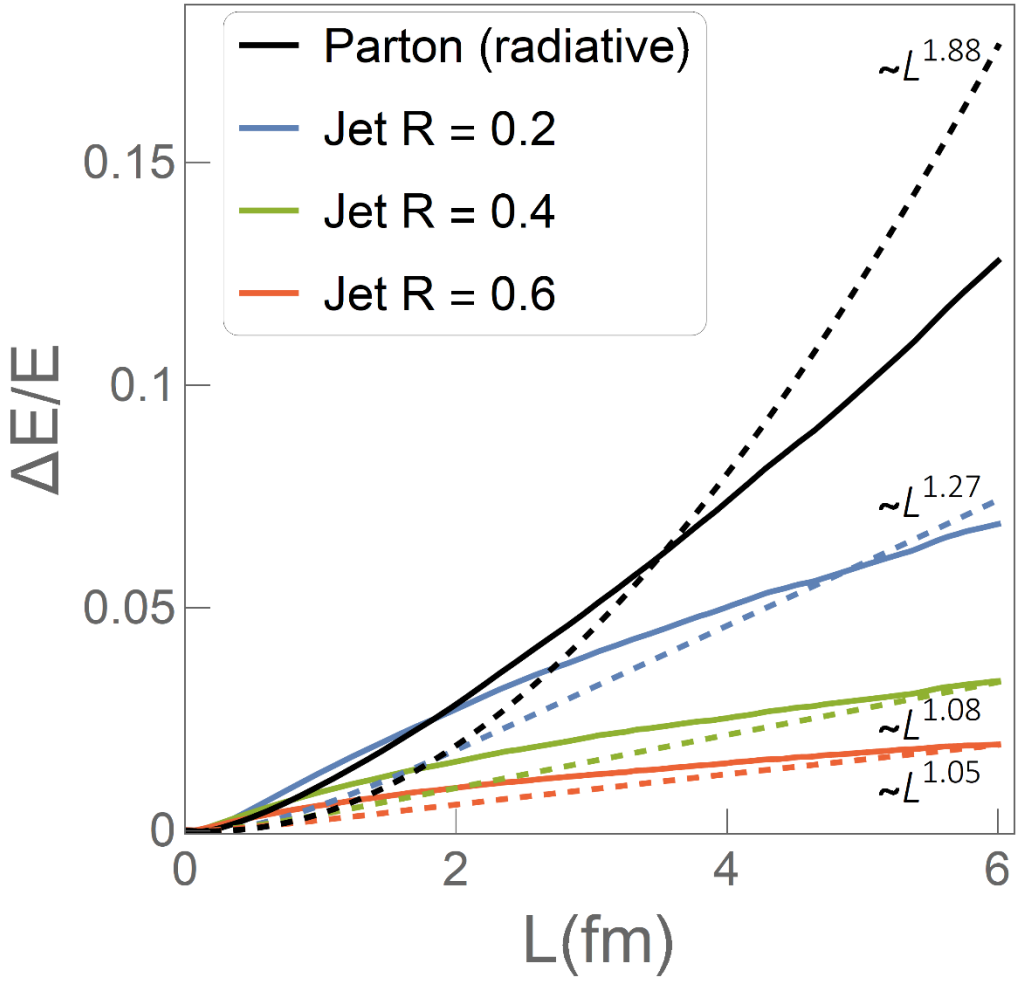

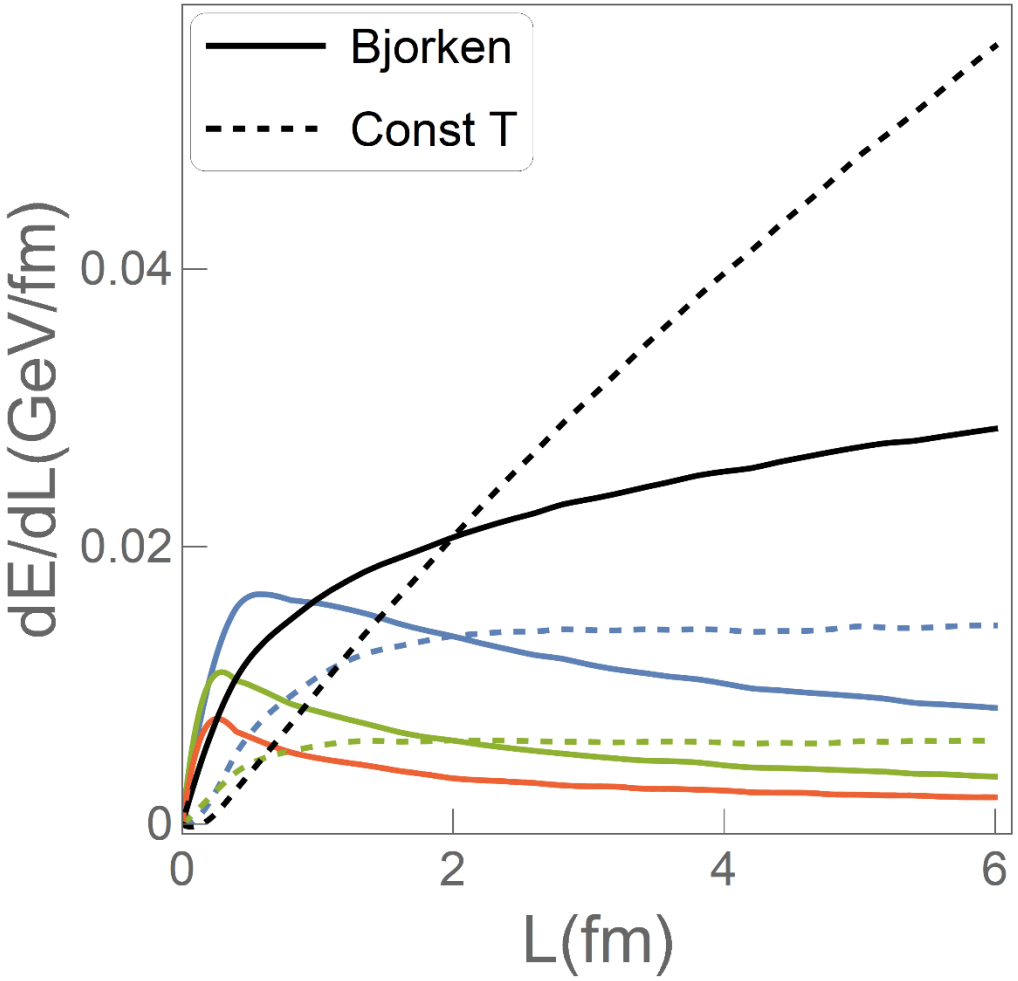

- Partonic radiative loss grows more strongly with L than the jet out-of-cone part.
- With increasing R, more induced radiation stays inside the cone, so jet energy loss shows a weaker L-dependence.
- Bjorken expansion further softens this LL-dependence relative to the static-brick case.

Energy loss in QGP

Energy loss in QGP

Radiative energy loss

Radiative energy loss comes from the processes in which there are more outgoing than incoming particles:

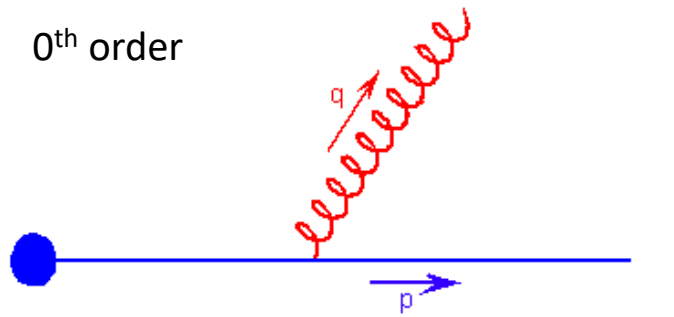

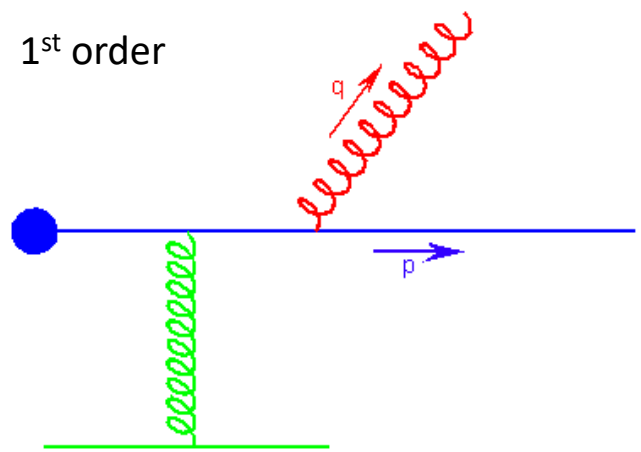

Collisional energy loss

Collisional energy loss comes from the processes which have the same number of incoming and outgoing particles:

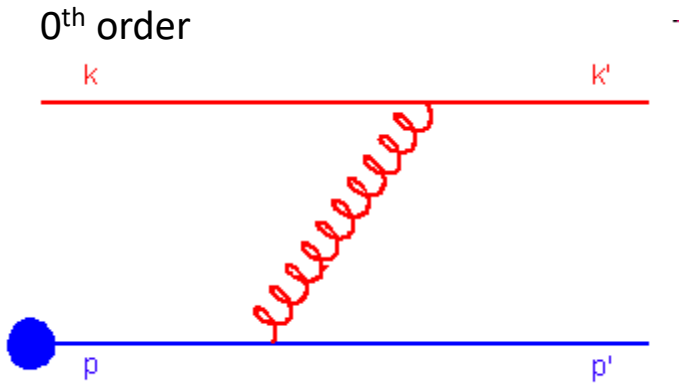

Energy loss in QGP

Radiative energy loss

Radiative energy loss comes from the processes in which there are more outgoing than incoming particles:

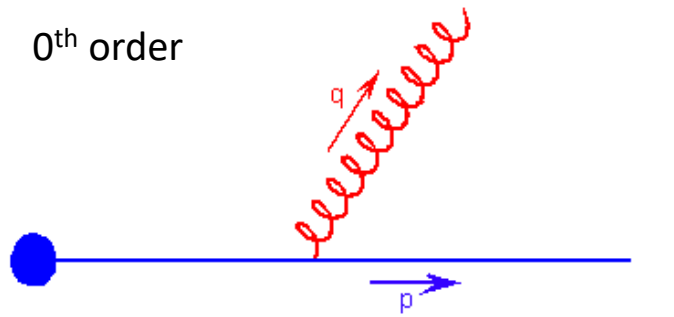

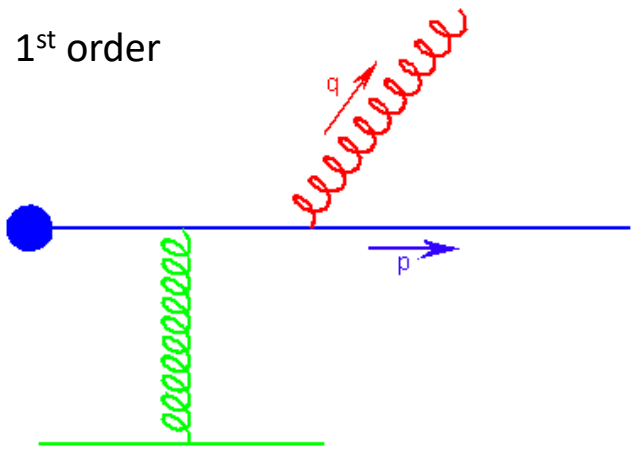

Collisional energy loss

Collisional energy loss comes from the processes which have the same number of incoming and outgoing particles:

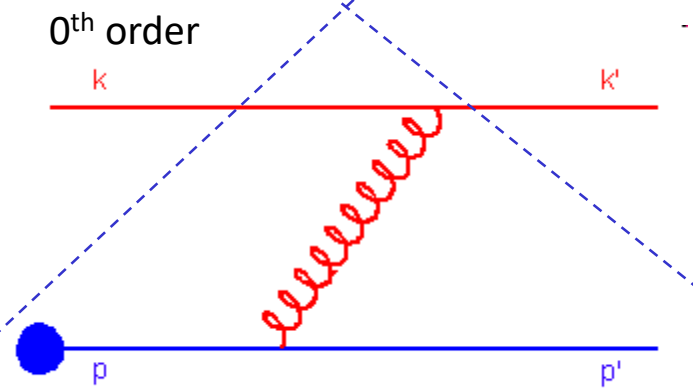

Considered to be negligible compared to radiative!

Heavy flavor puzzle @ RHIC

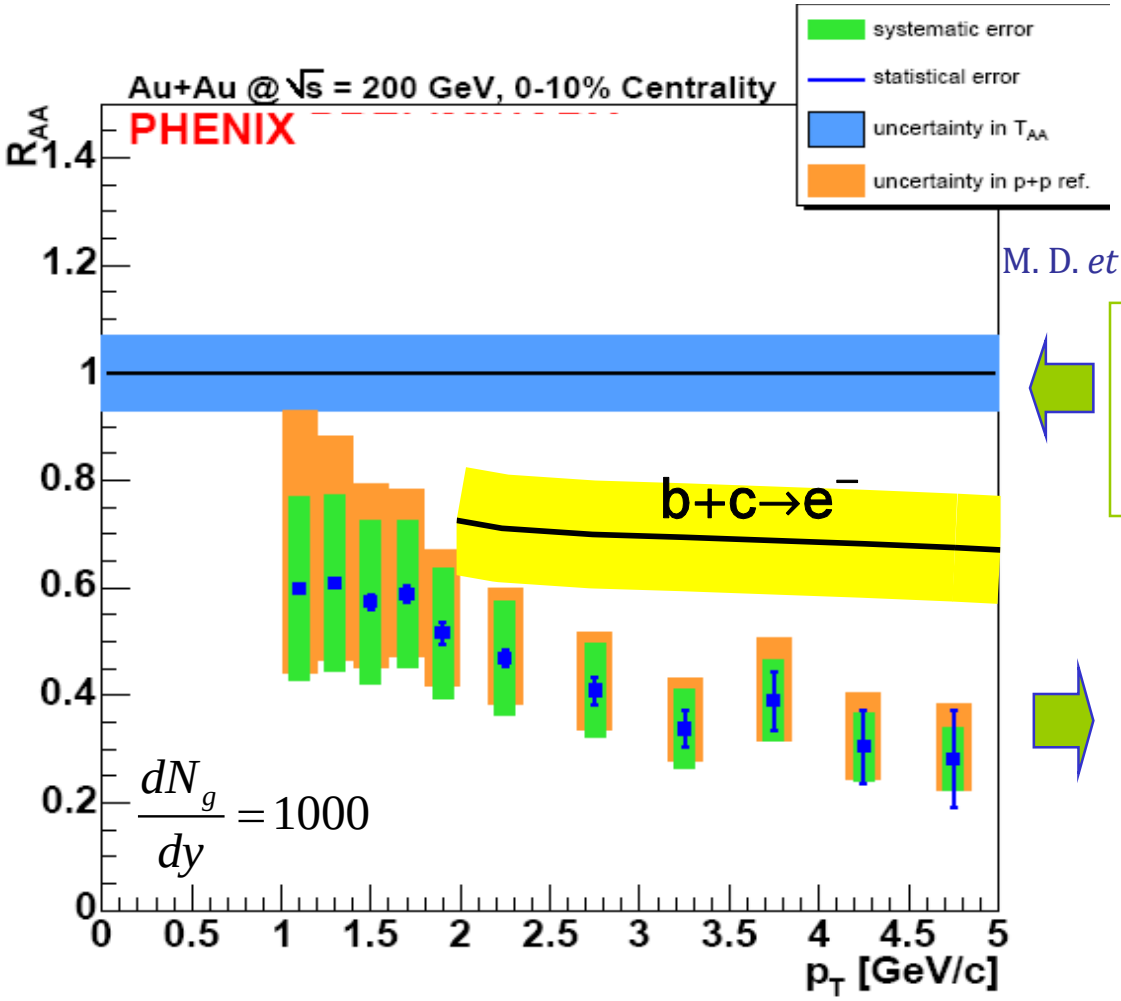

M. D. *et al.*, Phys. Lett. B 632, 81 (2006)

Radiative energy loss predictions with $dN_g/dy=1000$

Disagreement!

Radiative energy loss cannot explain the single electron data as long as realistic parameter values are considered!

Does the radiative energy loss control the energy loss in QGP?

Is collisional energy loss also important?

Collisional energy loss in a finite size QCD medium

Consider a medium of size L in thermal equilibrium at temperature T.

The main order collisional energy loss is determined from:

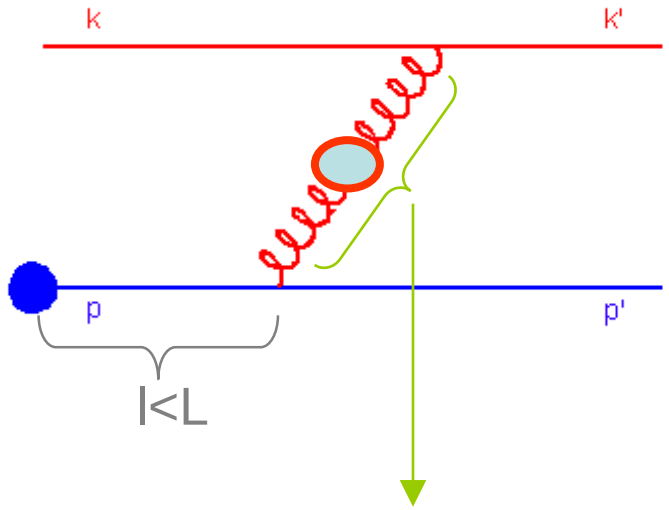

The effective gluon propagator:

$$D^{\mu\nu}(\omega,\vec{\mathrm{q}}) = -P^{\mu\nu}\Delta_T(\omega,\vec{\mathrm{q}}) - Q^{\mu\nu}\Delta_L(\omega,\vec{\mathrm{q}})$$

M. D., Phys.Rev.C74:064907,2006

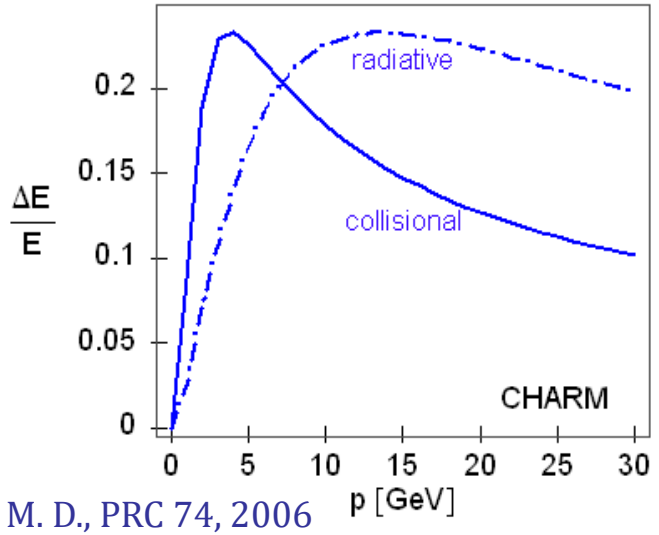

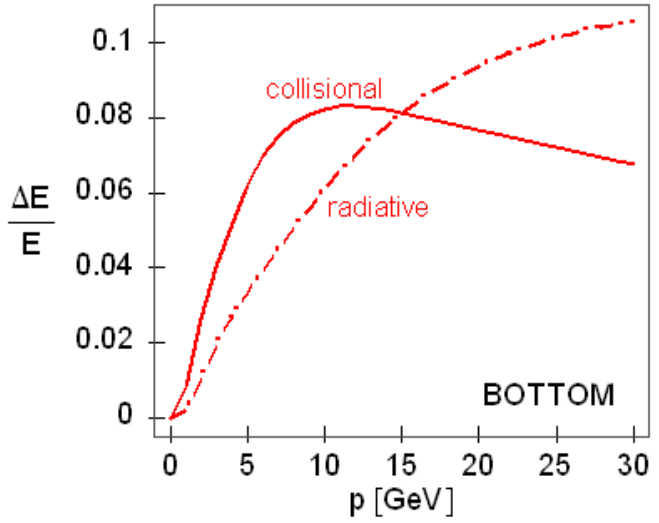

M. D., PRC 74, 2006

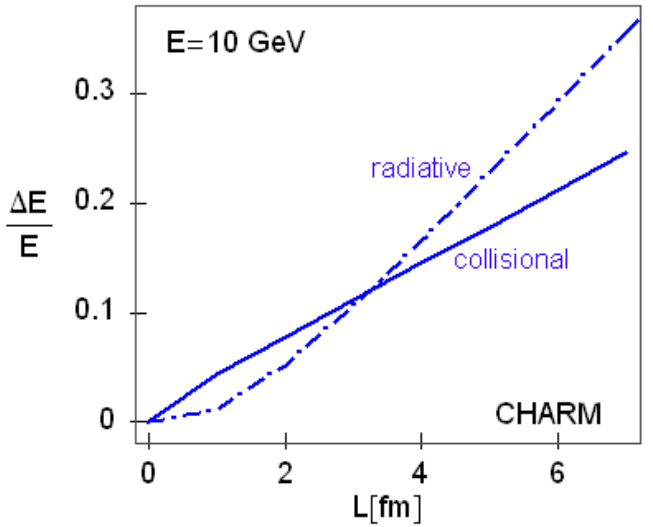

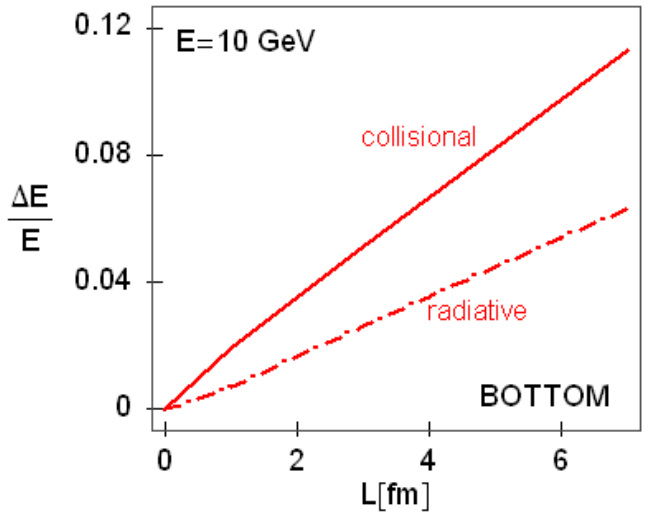

Collisional and radiative energy losses are comparable!

Non-zero collisional energy loss - a fundamental problem

Static QCD medium approximation (modeled by Yukawa potential).

With such approximation, collisional energy loss has to be exactly equal to zero!

However, collisional and radiative energy losses are shown to be comparable.

Introducing collisional energy loss is necessary but inconsistent with static approximation!

Static medium approximation should not be used in radiative energy loss calculations!

Dynamical QCD medium effects have to be included!

Our goal

Compute the light and heavy quark radiative energy loss in a dynamical medium of thermally distributed massless quarks and gluons.

Why?

- Address the applicability of static approximation in radiative energy loss computations.
- Compute collisional and radiative energy losses within a consistent theoretical framework.

Radiative energy loss in a dynamical medium

Compute the medium-induced radiative energy loss for a heavy quark to the first (lowest) order in the number of scattering centers.

Consider the radiation of one gluon induced by one collisional interaction with the medium.

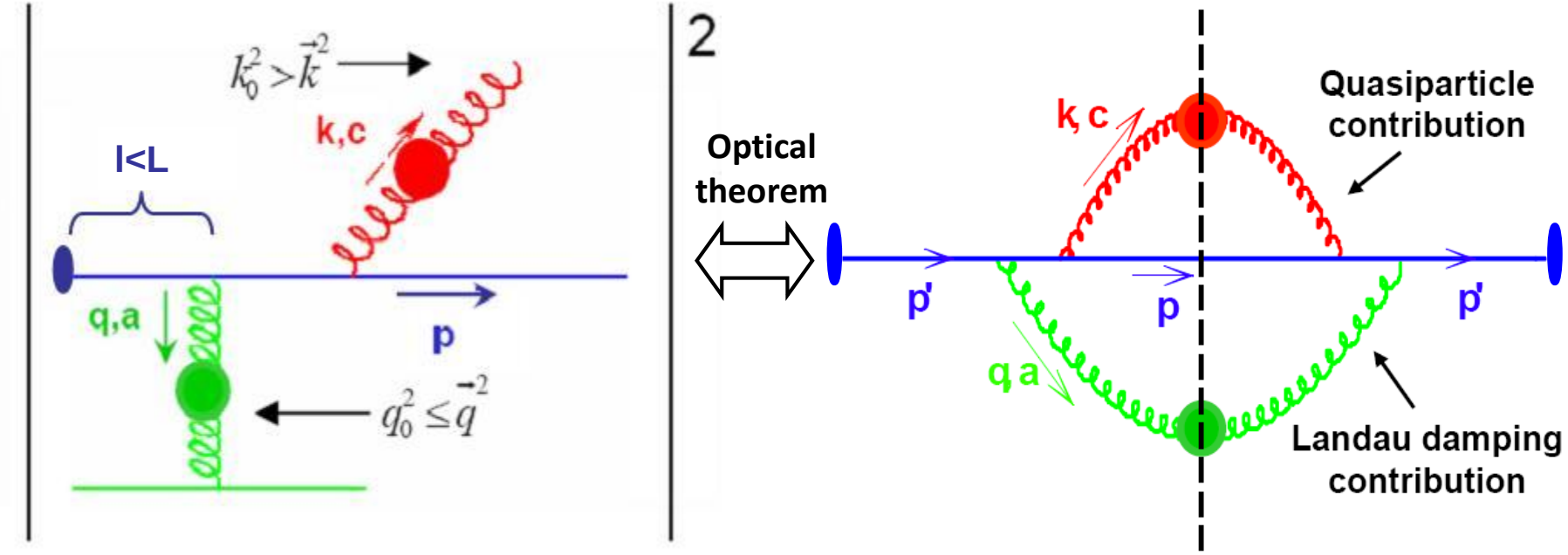

Consider a medium of finite size L, and assume that the collisional interaction has to occur in the medium.

The calculations were performed by using two Hard-Thermal Loop approach.

1-HTL gluon propagator:

$$iD^{\mu\nu}(l) = \frac{P^{\mu\nu}(l)}{l^2 - \Pi_T(l)} + \frac{Q^{\mu\nu}(l)}{l^2 - \Pi_L(l)}$$

Cut 1-HTL gluon propagator:

$$D^{>}_{\mu\nu}(l) = -(1+f(l_0))\Big(P_{\mu\nu}(l)\rho_T(l) + Q_{\mu\nu}(l)\rho_L(l)\Big)\,,$$

$$\rho_{L,T}(l) = \underbrace{2\pi\,\delta(l^2 - \Pi_{T,L}(l))}_{\text{Radiated gluon}} - \underbrace{2\,\mathrm{Im}\left(\frac{1}{l^2 - \Pi_{T,L}(l)}\right)\theta(1 - \frac{l_0^2}{\vec{l}^2})}_{\text{Exchanged gluon}}$$

For radiated gluon, the cut 1-HTL gluon propagator can be simplified to

(M.D. and M. Gyulassy, PRC 68, 034914 (2003))

$$D^{>}_{\mu\nu}(k) \approx -2\pi\,\frac{P_{\mu\nu}(k)}{2\omega}\,\delta(k_0 - \omega) \qquad \omega \approx \sqrt{\vec{k}^2 + m_g^2}\,; \quad m_g \approx \mu/\sqrt{2}$$

For exchanged gluon, the cut 1-HTL gluon propagator cannot be simplified, since both transverse (magnetic) and longitudinal (electric) contributions will prove to be important.

$$D^{>}_{\mu\nu}(q) = \theta(1 - \frac{q_0^2}{\vec{q}^2})\,(1 + f(q_0))\,2\,\mathrm{Im}\left(\frac{P_{\mu\nu}(q)}{q^2 - \Pi_T(q)} + \frac{Q_{\mu\nu}(q)}{q^2 - \Pi_L(q)}\right)$$

More than one cut of a Feynman diagram can contribute to the energy loss in finite-size dynamical QCD medium:

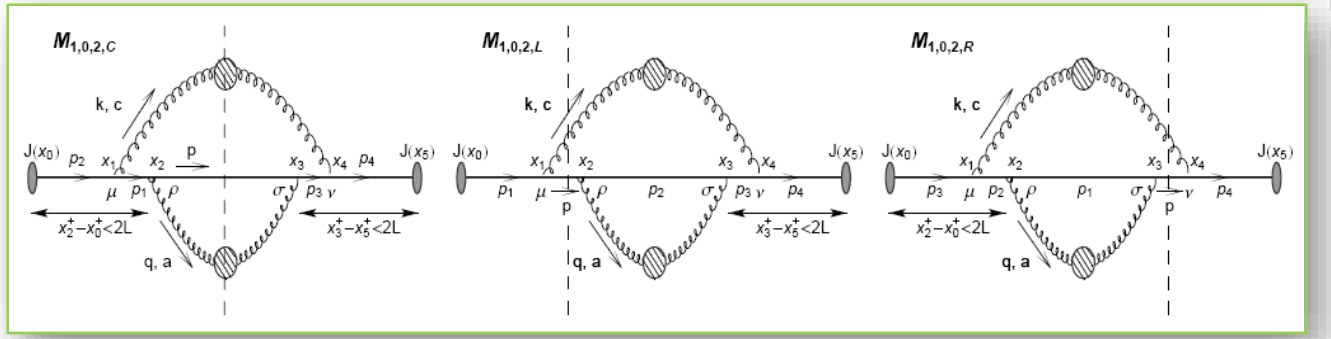

These terms interfere with each other, leading to the nonlinear dependence of the jet energy loss.

M. D., Phys.Rev.C80:064909,2009 (highlighted in APS Physics).

We calculated all the relevant diagrams that contribute to this energy loss.

Each individual diagram is infrared divergent due to the absence of magnetic screening!

The divergence is naturally regulated when all the diagrams are taken into account.

So, all 24 diagrams have to be included to obtain a sensible result.

$$\frac{\Delta E_{\rm dyn}}{E} = \frac{C_R\alpha_s}{\pi}\frac{L}{\lambda_{\rm dyn}}\int dx\,\frac{d^2k}{\pi}\frac{d^2q}{\pi}\frac{\mu^2}{q^2(q^2+\mu^2)}\left(1-\frac{\sin\frac{(k+q)^2+\chi}{xE^+}L}{\frac{(k+q)^2+\chi}{xE^+}L}\right)$$
$$\times 2\frac{(k+q)}{(k+q)^2+\chi}\left(\frac{(k+q)}{(k+q)^2+\chi}-\frac{k}{k^2+\chi}\right),$$

The dynamical energy loss formalism

Has the following unique features:

- *Finite size finite temperature* QCD medium of *dynamical* (moving) partons
- Based on finite T field theory and generalized HTL approach
- Same theoretical framework for both radiative and collisional energy loss
- Applicable to both light and heavy flavor.
- Finite magnetic mass effects
  (M. D. and M. Djordjevic, PLB 709:229 (2012))
- Running coupling
  (M. D. and M. Djordjevic, PLB 734, 286 (2014)).
- Relaxed soft-gluon approximation
  (B. Blagojevic, M. D. and M. Djordjevic, PRC 99, 024901, (2019)).
- All ingredients necessary to accurately explain the data
  (B. Blagojevic and M.D, J.Phys. G42 (2015) 7, 075105).
- No fitting parameters in the model
- Temperature as a natural variable in the model.

Numerical procedure

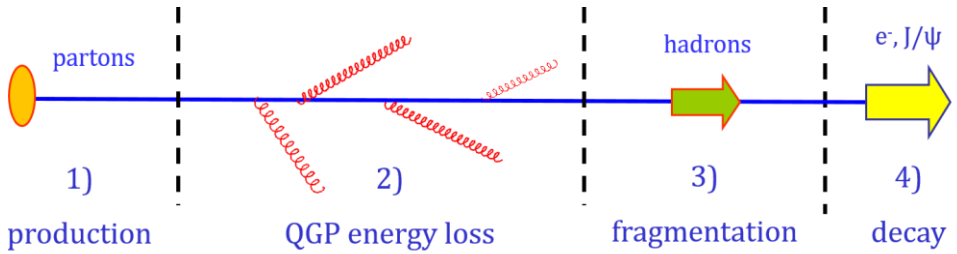

- Light flavor production
  Z.B. Kang, I. Vitev, H. Xing, PLB 718:482 (2012)
- Heavy flavor production
  M. Cacciari et al., JHEP 1210, 137 (2012)
- Path-length fluctuations A. Dainese, EPJ C33:495,2004.
- Multi-gluon fluctuations
  M. Gyulassy, P. Levai, I. Vitev, PLB 538:282 (2002).
- DSS and KKP fragmenation for light flavor
  D. de Florian, R. Sassot, M. Stratmann, PRD 75:114010 (2007)
  B. A. Kniehl, G. Kramer, B. Potter, NPB 582:514 (2000)
- BCFY and KLP fragmenation for heavy flavor
  M. Cacciari, P. Nason, JHEP 0309: 006 (2003)
- Decays of heavy mesons to single e and J/ψ
  M. Cacciari et al., JHEP 1210, 137 (2012)
- T=304MeV for LHC and T=221MeV for RHIC.
  M. Wilde, Nucl. Phys. A 904-905, 573c (2013) (ALICE)
  A. Adare *et al.*, Phys. Rev. Lett. 104, 132301 (2010) (PHENIX)

QGP discovered at LHC and RHIC.

A current goal: Understand QGP properties

Expected: The QGP was anticipated to behave as a weakly interacting gas.

Current paradigm:

- Strongly coupled system, i.e., nearly perfect fluid.
- Estimated η/s close to the lower bound conjectured by AdS/CFT.

Surprising connection between the hottest and coldest matter on Earth.

M. A. Lisa, *et al.*, New J. Phys. 13 (2011)

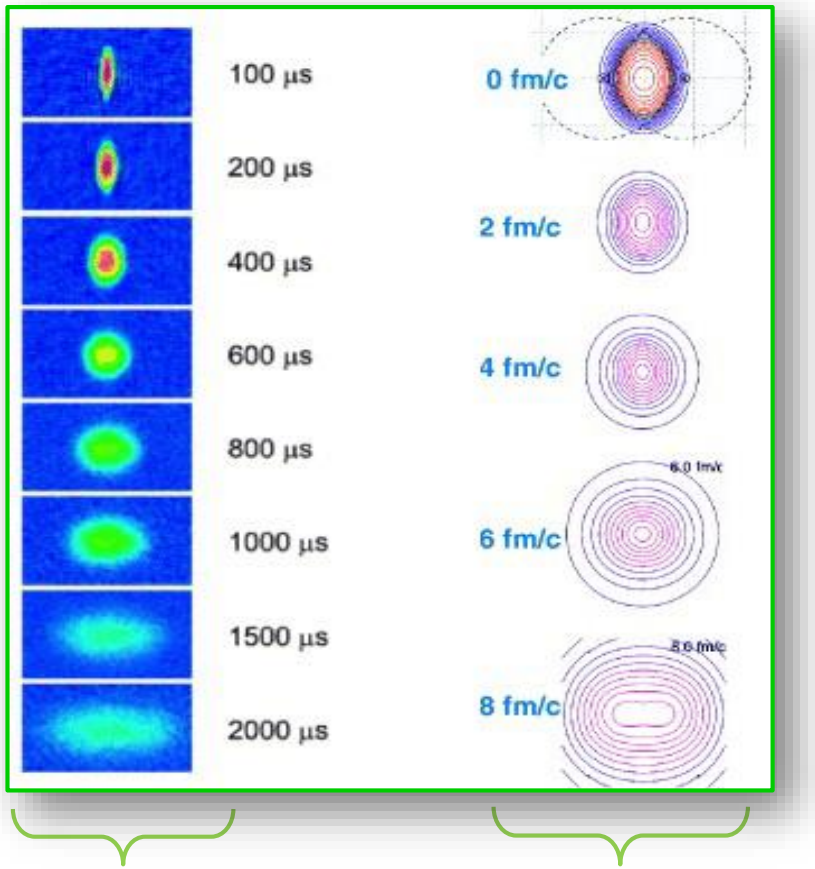

Ultracold Fermi gas $T \sim 10^{-6}$K

perfect fluid QGP simulation $T \sim 10^{12}$K

Is QGP really perfect fluid?

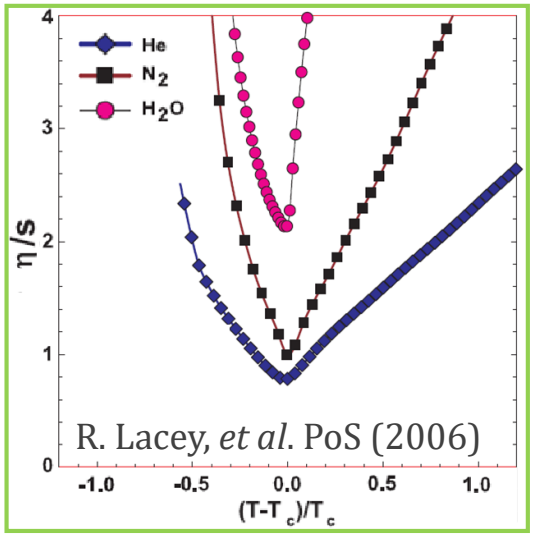

Origin of the low η/s throughout QGP evolution unclear.

η/s increases with T for all other substances.

The paradigm originates from the relativistic hydrodynamics.

H. Niemi *et al.*, PRL 106 (2011)

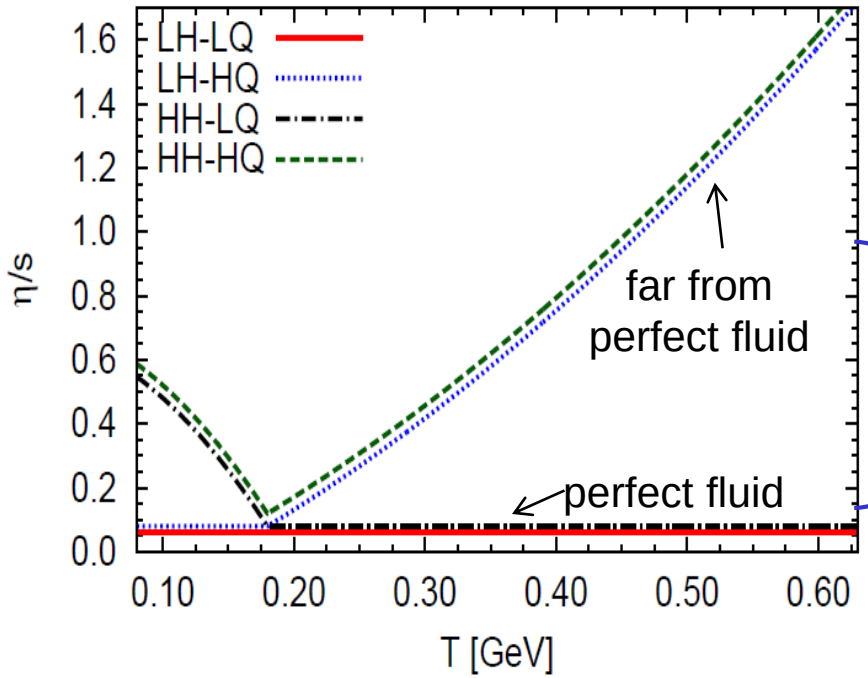

However, the predictions insensitive to even a large increase in η/s not far away from the transition temperature (T_c).

Similar insensitivity by other approaches, e.g.:

- hydro (PRC 94:024907,2016)
- parton transport (PRC 92:054902,2015)

Perfect fluid too perfect ?

J. Nagle *et al.*, New J.Phys.13:075004,2011

Relativistic hydrodynamics predictions → Low momentum data

How to provide substantially new insight?

pQCD predictions → High momentum (pt) data

The main idea: Use high pt data/theory

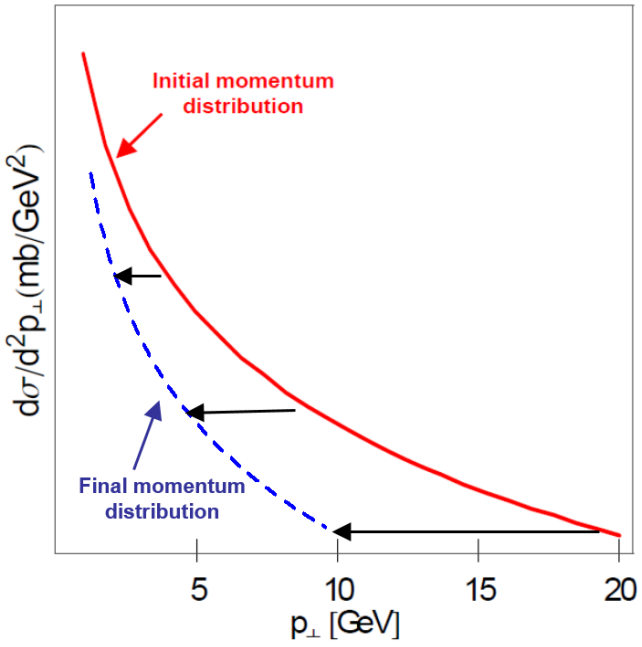

$$R_{AA} = \frac{\text{Final momentum distribution}}{\text{Initial momentum distribution}}$$

Wealth of precision high pt data available, or will soon become available - dawn of the high precision era (Run3 at the LHC and sPHENIX at BNL).

Angular *average* suppression
high pt hadron R_{AA}

Probes high *pt* parton interactions with QGP

Angular *differential* suppression
high pt hadron v_2 and higher harmonics

Probes QGP evolution

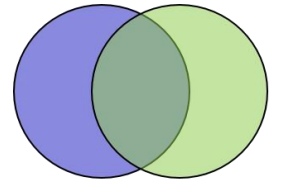

Assymetric collision of two heavy ions

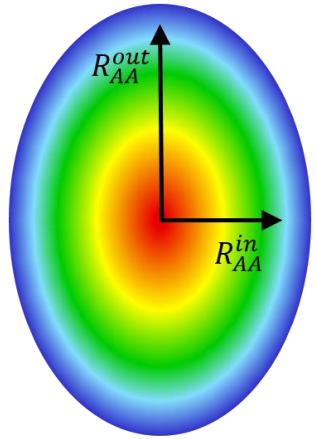

$$v_2 = \frac{R_{AA}^{in} - R_{AA}^{out}}{R_{AA}^{in} + R_{AA}^{out}}$$

The main idea behind high-pt QGP tomography

Different *bulk* medium parameters lead to different $T(\vec{x},\phi)$

Directly probe T profiles through high *pt* partons

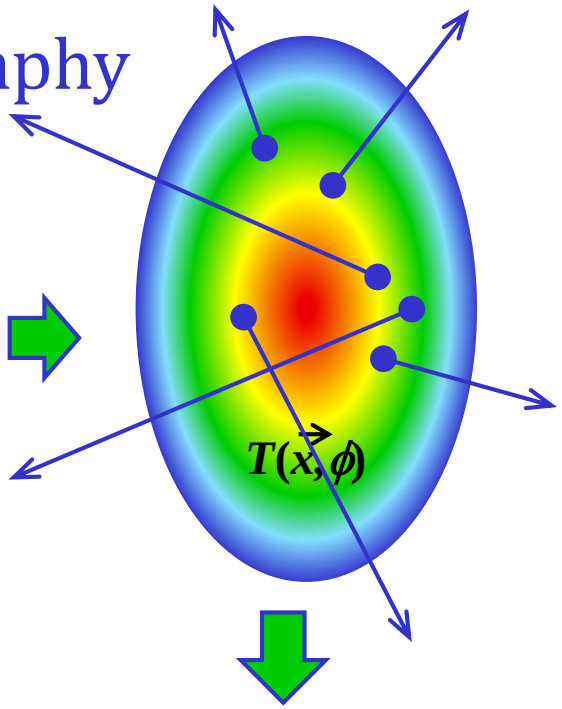

Compare with high *pt* data for both *light and heavy* flavour probes

Infer $T(\vec{x},\phi)$ (i.e. $\eta/s(T)$) consistent with both low-*pt* and high-*pt* data

Note: Contribution to the energy loss is larger for higher T

Larger sensitivity for inferring η/s at high T

In distinction to low pt data which are the least sensitive at high T

High *pt* theory/data – powerful complementary tool to constrain bulk QGP properties.